Calhoun: The NPS Institutional Archive

DSpace Repository

Theses and Dissertations | 1. Thesis and Dissertation Collection, all items

1987-12

Changes in the California current system observed off northern California during July-August 1986

Beasley, Michael E.

Monterey, California. Naval Postgraduate School

http://hdl.handle.net/10945/22662

This publication is a work of the U.S. Government as defined in Title 17, United States Code, Section 101. Copyright protection is not available for this work in the United States.

Downloaded from NPS Archive: Calhoun

http://www.nps.edu/library

Calhoun is the Naval Postgraduate School's public access digital repository for research materials and institutional publications created by the NPS community. Calhoun is named for Professor of Mathematics Guy K. Calhoun, NPS's first appointed -- and published -- scholarly author.

Dudley Knox Library / Naval Postgraduate School
411 Dyer Road / 1 University Circle
Monterey, California USA 93943

NPS 68-88-002

NAVAL POSTGRADUATE SCHOOL

Monterey, California

B3145

THESIS

CHANGES IN THE CALIFORNIA CURRENT SYSTEM
OBSERVED OFF NORTHERN CALIFORNIA
DURING JULY-AUGUST 1986

by

Michael E. Beasley

December 1987

Thesis Advisor M.L. Batteen

Approved for public release; distribution is unlimited

Prepared for:

Chief of Naval Research
800 N. Quincy St.
Arlington, VA 22217-5000

T238692

NAVAL POSTGRADUATE SCHOOL
Monterey, California

Rear Admiral R. C. Austin
Superintendent

K. T. Marshall
Acting Provost

This thesis was prepared in conjunction with research sponsored by the Naval Postgraduate School Research Foundation.

Reproduction of all or part of this report is authorized.

Released by:

REPORT DOCUMENTATION PAGE

1a REPORT SECURITY CLASSIFICATION UNCLASSIFIED	1b RESTRICTIVE MARKINGS
2a SECURITY CLASSIFICATION AUTHORITY	3 DISTRIBUTION AVAILABILITY OF REPORT Approved for public release; Distribution is unlimited.
2b DECLASSIFICATION / DOWNGRADING SCHEDULE	
4 PERFORMING ORGANIZATION REPORT NUMBER(S) NPS 68-88-002	5 MONITORING ORGANIZATION REPORT NUMBER(S)
6a NAME OF PERFORMING ORGANIZATION Naval Postgraduate School 6b OFFICE SYMBOL (If applicable) 68	7a NAME OF MONITORING ORGANIZATION Naval Postgraduate School
6c ADDRESS (City, State, and ZIP Code) Monterey, California 93943-5000	7b ADDRESS (City, State, and ZIP Code) Naval Postgraduate School Research Foundation Monterey, California 93943-5000
8a NAME OF FUNDING / SPONSORING ORGANIZATION NPS Research Foundation 8b OFFICE SYMBOL (If applicable)	9 PROCUREMENT INSTRUMENT IDENTIFICATION NUMBER N0001487WR4E011
8c ADDRESS (City, State, and ZIP Code) Naval Postgraduate School Monterey, California 93943-5000	10 SOURCE OF FUNDING NUMBERS PROGRAM ELEMENT NO: 61153N PROJECT NO: RR014-01 TASK NO: 10P-011 WORK UNIT ACCESSION NO:
11 TITLE (Include Security Classification) Changes in the California Current System Observed Off Northern California During July-August 1986	
12 PERSONAL AUTHOR(S) Beasley, Michael E. in conjunction with M. L. Batteen and C. N. K. Mooers.	
13a TYPE OF REPORT Master's Thesis 13b TIME COVERED FROM _____ TO _____ 14 DATE OF REPORT (Year, Month, Day) December 1987 15 PAGE COUNT 72	
16 SUPPLEMENTARY NOTATION	
17 COSATI CODES FIELD / GROUP / SUB-GROUP	18 SUBJECT TERMS (Continue on reverse if necessary and identify by block number) California Current System description - 1986, Upwelling, CCS jets

19 ABSTRACT (Continue on reverse if necessary and identify by block number)

Changes in the flow pattern of the California Current System (CCS) in a relatively short time period (~ one week) are investigated. The offshore flow pattern changed orientation from southwestward to southward and a cool filament seen previously was no longer discernible. The nearshore flow pattern changed from a predominantly southward to a northward flow. The changes occurred between two OPTOMA cruises conducted in the summer of 1986. Two possible causes are investigated for these changes: 1) a change in the poleward undercurrent of the CCS, and 2) a change in the coastal winds. Analysis of cross-sections of the poleward undercurrent indicate that it remained subsurface throughout the cruises. Analysis of wind data indicate that southward winds were the dominant wind pattern throughout the first cruise. Wind data from a moored buoy off Point Arena indicate northward winds (i.e., wind reversals) following the first cruise, which could be associated with the changes in the flow patterns of the CCS.

20 DISTRIBUTION / AVAILABILITY OF ABSTRACT ☒ UNCLASSIFIED/UNLIMITED ☐ SAME AS RPT ☐ DTIC USERS	21 ABSTRACT SECURITY CLASSIFICATION UNCLASSIFIED
22a NAME OF RESPONSIBLE INDIVIDUAL M. L. Batteen	22b TELEPHONE (Include Area Code) (408) 646-3265 22c OFFICE SYMBOL 68Bv

DD FORM 1473, 84 MAR — 83 APR edition may be used until exhausted. All other editions are obsolete.

SECURITY CLASSIFICATION OF THIS PAGE

☆ U.S. Government Printing Office: 1986—606-24.

Approved for public release; distribution is unlimited.

Changes in the California Current System observed off Northern California during July-August 1986

by

Michael E. Beasley
Lieutenant, United States Navy
B.S., Auburn University, 1979

Submitted in partial fulfillment of the
requirements for the degree of

MASTER OF SCIENCE IN METEOROLOGY AND OCEANOGRAPHY

from the

NAVAL POSTGRADUATE SCHOOL
December 1987

ABSTRACT

Changes in the flow pattern of the California Current System (CCS) in a relatively short time period ($\sim$ one week) are investigated. The offshore flow pattern changed orientation from southwestward to southward and a cool filament seen previously was no longer discernible. The nearshore flow pattern changed from a predominantly southward to a northward flow. The changes occurred between two OPTOMA cruises conducted in the summer of 1986. Two possible causes are investigated for these changes: 1) a change in the poleward undercurrent of the CCS, and 2) a change in the coastal winds. Analysis of cross-sections of the poleward undercurrent indicate that it remained subsurface throughout the cruises. Analysis of wind data indicate that southward winds were the dominant wind pattern throughout the first cruise. Wind data from a moored buoy off Point Arena indicate northward winds (i.e., wind reversals) following the first cruise, which could be associated with the changes in the flow patterns of the CCS.

Thesis
B3145
c.1

TABLE OF CONTENTS

I. INTRODUCTION 8
A. OBJECTIVES 8
B. STUDY AREA 8
C. BACKGROUND 9
1. Historical Notes on Atmospheric Forcing and the CCS 9
2. Previous Data Collections in the CCS 10

II. DATA ACQUISITION AND DESCRIPTION 12
A. DATA ACQUISITION 12
1. OPTOMA Cruise Data 12
2. Other Data Acquired 14
B. THE OBJECTIVE ANALYSIS TECHNIQUE 21

III. RESULTS 22
A. SATELLITE IMAGERY 22
B. WIND DATA 22
C. ANALYSIS OF HYDROGRAPHIC DATA 29
1. OPTOMA 21 29
2. OPTOMA 22 46
3. Coastal Flow 61

IV. CONCLUSIONS AND RECOMMENDATIONS 64
A. CONCLUSIONS 64
B. RECOMMENDATIONS 64

LIST OF REFERENCES 67

INITIAL DISTRIBUTION LIST 69

DUDLEY KNOX LIBRARY
NAVAL POSTGRADUATE SCHOOL

LIST OF FIGURES

1.1 OPTOMA NOCAL and CENCAL subdomains and the CODE domain. Isobaths are shown in meters. 10
2.1 Ship track for OPTOMA 21 from Wittmann *et al.*, 1987 13
2.2 OPTOMA 21 sea surface temperature field. The contour interval is 0.5°C 14
2.3 Ship track for OPTOMA 22 from Ciandro *et al.*, 1986 15
2.4 OPTOMA 22 Sea surface temperature field The contour interval is 0.5°C 17
2.5 Relative positions of NDBC 14 (shown by the circle) and of the Bakun upwelling index (shown by the square) 18
2.6 Buoy winds at 39.2°N, 124.0°W during the OPTOMA cruises 19
2.7 The Bakun Upwelling Index for the period 1 March through 28 August, 1986 20
3.1 NOAA-9 satellite IR image, 18 June, 1986 23
3.2 NOAA-9 satellite IR image, 14 July, 1986 24
3.3 NOAA-9 satellite IR image, 16 July, 1986 25
3.4 NOAA-9 satellite IR image, 17 July, 1986 26
3.5 NOAA-9 satellite IR image, 29 July, 1986 27
3.6 NOAA-9 satellite IR image, 30 July, 1986 28
3.7 Poleward winds following the OPTOMA 21 cruise 12Z 22 July, 1986. Arrow denotes NDBC 14. 30
3.8 Cessation of poleward winds immediately following the OPTOMA 21 cruise, 06Z 23 July, 1986 31
3.9 Start of poleward winds prior to OPTOMA 22 cruise 18Z 24 July, 1986 32
3.10 Cessation of poleward winds prior to OPTOMA 22 cruise 00Z 27 July, 1986 33
3.11 Start of poleward winds during the OPTOMA 22 cruise 12Z 28 July, 1986 34
3.12 OPTOMA 21 (A) Surface dynamic topography and (B) Surface geostrophic currents 36

3.13 OPTOMA 21 (A) 50 m depth dynamic topography and (B) 50 m depth geostrophic currents 37
3.14 OPTOMA 21 (A) 100 m Dynamic Height Topography and (B) 100 m geostrophic currents 38
3.15 OPTOMA 21 (A) 150 m dynamic topography and (B) 150 m geostrophic currents 40
3.16 OPTOMA 21 (A) 200 m dynamic topography and (B) 200 m geostrophic currents 41
3.17 OPTOMA 21 (A) 250 m dynamic topography and (B) 250 m geostrophic currents 42
3.18 OPTOMA 21 nearshore temperature-salinity diagram 43
3.19 OPTOMA 21 offshore temperature-salinity diagram 44
3.20 Survey stations for OPTOMA 21 (from Wittmann *et al.*, 1987) and the two vertical cross sections 45
3.21 OPTOMA 21 vertical cross sections along the jet (A) Temperature and (B) Salinity 47
3.22 OPTOMA 21 vertical cross sections across the jet (A) Temperature and (B) Salinity 48
3.23 OPTOMA 22 (A) Surface dynamic topography and (B) Surface geostrophic currents 50
3.24 OPTOMA 22 (A) 50 m dynamic topography and (B) 50 m geostrophic currents 51
3.25 OPTOMA 22 (A) 100 m dynamic topography and (B) 100 m geostrophic currents 53
3.26 OPTOMA 22 (A) 150 m dynamic topography and (B) 150 m geostrophic currents 54
3.27 OPTOMA 22 (A) 200 m dynamic topography and (B) 200 m geostrophic currents 55
3.28 OPTOMA 22 (A) 250 m dynamic topography and (B) 250 m geostrophic currents 56
3.29 OPTOMA 22 offshore temperature-salinity diagram 57
3.30 OPTOMA 22 stations and the vertical cross sections (from Ciandro *et al.*, 1986) 58
3.31 OPTOMA 22 temperature vertical cross section at E-F 59
3.32 OPTOMA 22 temperature vertical cross section at G-H 60
3.33 OPTOMA 22 temperature vertical cross section at I-J 62
3.34 OPTOMA 22 temperature vertical cross section at K-L 63

ACKNOWLEDGEMENTS

The professional guidance, patience, and support of my advisor, Dr. Mary L. Batteen and second reader Dr. Christopher N.K. Mooers, have been an essential and invaluable part of this thesis. Dr. Mooers allowed me to participate in the OPTOMA 22 cruise, which led to this thesis. Dr. Batteen continually guided me along in this endeavor. Ms. Melissa Ciandro, currently at the Scripps Satellite Oceanography Facility, was invaluable due to her expertise in computer programming and satellite imagery.

Much of the credit in the completion of this thesis is due to my wife and children, Cary, William, and Rebecca, who continually gave their time and loving support throughout.

I. INTRODUCTION

A. OBJECTIVES

Recently, an oceanographic cruise was conducted in the waters off northern California that yielded unexpected results. OPTOMA 22, an oceanographic cruise, was conducted 27 July through 5 August, 1986. The purpose of the cruise was to define an offshore flowing jet mapped by OPTOMA 21, a cruise that ended seven days earlier. What was seen though, was a different dynamical structure than was expected. The offshore flowing jet of OPTOMA 21 was no longer present and the general flow was now oriented parallel to the coast instead of perpendicular to the coast. The nearshore flow pattern also changed from southward to northward. What happened over such a relatively small time scale to change the structure of the flow field?

The primary objectives of this thesis are to describe the flow fields during both cruises and also systematically investigate what caused the changes in the flow fields off northern California seen in OPTOMA 22. Two possible reasons for these changes which could well be coupled are: 1) a significant decline or change in the winds favorable for upwelling; and 2) a change in the state of the poleward California Undercurrent.

The organization of this paper is as follows. I will first present background information on the general features and discuss recent data acquired in surveys prior to OPTOMA 22 (from the CODE and OPTOMA programs). Next, I will describe the various types of data acquired and how they are used in my analysis (Chapter II). I will then show the results of the data analysis (Chapter III). Finally I will discuss my results, present conclusions and discuss very briefly some areas that might be covered by future research (Chapter IV).

B. STUDY AREA

The study domain for OPTOMA 22, NOCAL, is the northern of two sub-domains of the Ocean Prediction Through Observations, Modeling and Analysis (OPTOMA) program and is located at about 37°N to 39°N, 124°W to 128°W (Figure 1.1). The domain is located south of the Mendocino Escarpment, is mostly offshore of the continental slope, and has an average water depth of ~3900 m. The region is well within the California Current System (CCS) regime, which is now known

to be a complex eastern boundary current system consisting of eddies, jets and filaments (Mooers and Robinson, 1984).

C. BACKGROUND

1. Historical Notes on Atmospheric Forcing and the CCS

a. Atmospheric Forcing

The North Pacific High is the forcing mechanism for the equatorward California Current and upwelling along North America's west coast (Huyer,1983). In the summer, the high is at its most northwest position, centered at about 38°N, 150°W. Simultaneously, the extreme western United States develops a thermal low resulting from the very warm solar heated surface. This sets up an offshore pressure gradient marked by equatorward winds. These winds cause an offshore transport of water in the Ekman layer (Huyer, 1983). Superimposed on these equatorward winds are atmospheric fluctuations of 2 - 20 days which can lead to wind events or relaxations (Halliwell and Allen, 1987).

b. The CCS

As a result of this atmospheric forcing, a broad equatorward flowing surface California Current is set up as an eastern boundary current of the Pacific Ocean subtropical gyre. This is the major current in the CCS. The other currents in the CCS are: 1) the poleward flowing Southern California Countercurrent located south of Point Conception in the California Bight; 2) a poleward flowing Davidson Current located north of Point Conception during the fall and winter; and 3) a California Undercurrent, also known as the Poleward Undercurrent or PUC (Kosro, 1987), that flows poleward in the vicinity of the continental slope and shelf (Hickey, 1979). Rienecker *et al.* (1985) ascertain that a synoptic look at the CCS will differ markedly from the classical notion that the CCS should have a broad, slow and shallow dynamic structure consistent with eastern boundary currents (Hickey, 1979). Recent observations have shown that the CCS contains numerous mesoscale eddies, meandering jets and turbulent filaments (Mooers and Robinson, 1984; Bernstein *et. al.*, 1977).

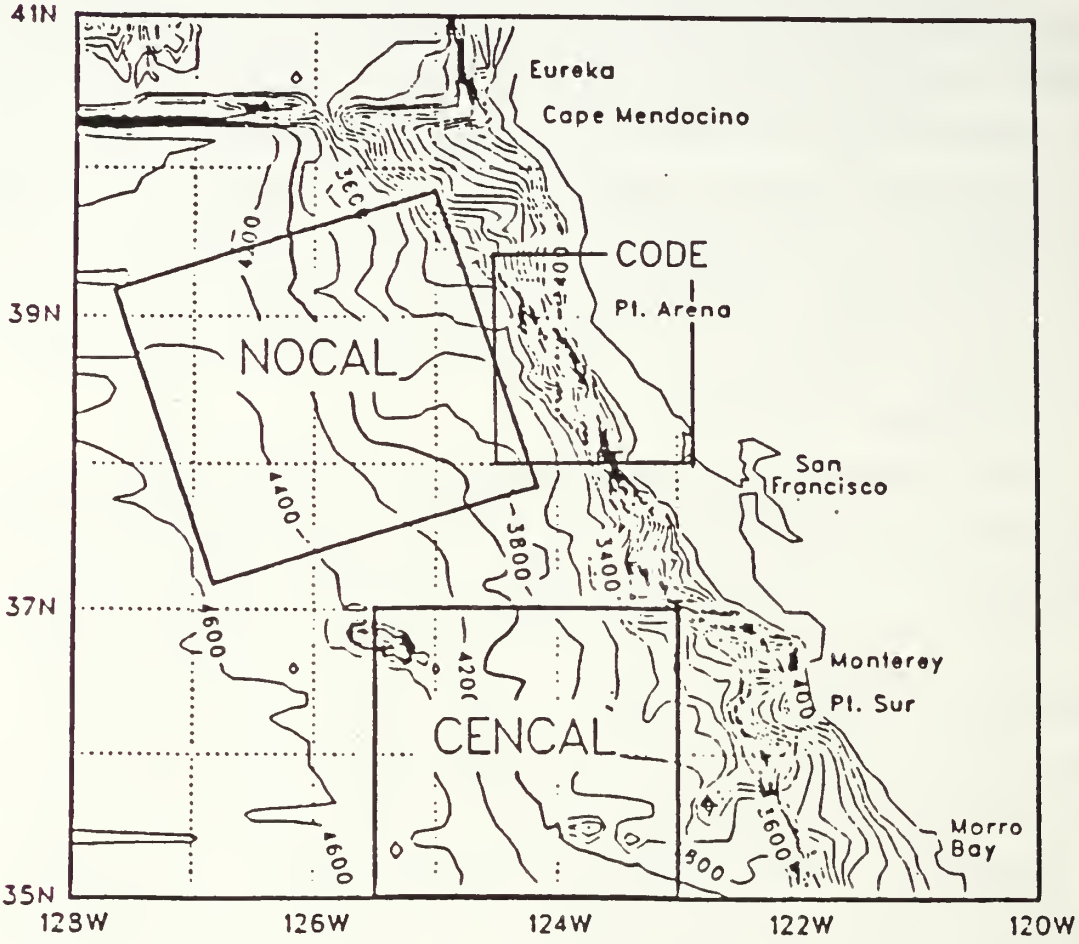

Figure 1.1 OPTOMA NOCAL and CENCAL subdomains and the CODE domain. Isobaths are shown in meters..

2. Previous Data Collections in the CCS

a. CALCOFI and CUE Programs

In 1949 the California Cooperative Fisheries Investigations (CALCOFI) program was initiated. Its main goal was to study fisheries variability associated with interannual variability in the CCS. These large-scale, long-term studies were conducted south of San Francisco, primarily between Point Conception at 35°N and Cabo San Lazaro at 25°N (Reid *et al.*, 1958).

About 1960, small scale studies of the coastal upwelling regime off Oregon were initiated (Huyer, 1983). Repeated sampling of a hydrographic section off Newport, Oregon was carried out, and in 1965 current meters were put in along the same section (Huyer, 1983). All of these upwelling study efforts culminated in the intensive Coastal Upwelling Experiments (CUE-I and CUE-II), which were carried out during the upwelling seasons (i.e., ~ March to September) of 1972 and 1973.

b. Data Analysis of the CODE Program

At the beginning of the OPTOMA program, the Coastal Ocean Dynamics Experiment (CODE) was finishing. It was conducted near the NOCAL domain (Figure 1.1) during the upwelling seasons of 1981 and 1982. The domain was in the area from Point Reyes (38°N, 123°W) to Point Arena (39°N, 123.7°W) with an offshore extent of ~50 km (Beardsley and Lentz, 1987; Zemba and Friehe, 1987). As seen in Figure 1.1, this area has a relatively straight coastline, simple and gradual bottom topography, and large wind stress fluctuations from winter to summer (Nelson, 1977).

c. Previous OPTOMA Surveys

Since 1982, the OPTOMA program has acquired observations in the NOCAL and CENCAL subdomains (see Figure 1.1). The cruises prior to OPTOMA 21 and OPTOMA 22, which were conducted during the summer, have documented upwelling, meandering jets, and mesoscale turbulent filaments (Rienecker *et al.*, 1985). These features seem to be typical features in the CCS occurring when equatorward winds dominate the atmospheric flow.

II. DATA ACQUISITION AND DESCRIPTION

A. DATA ACQUISITION

1. OPTOMA Cruise Data

Both OPTOMA 21 and 22 were part of a research program sponsored by the Office of Naval Research. The OPTOMA program was conceived to try to understand the mesoscale (fronts, eddies and jets) variability and dynamics of the CCS and to determine the scientific limits to practical mesoscale ocean forecasting. The general OPTOMA domain was off the California coast, with two subdomains being extensively sampled, NOCAL and CENCAL (Figure 1.1). The NOCAL subdomain was covered in both OPTOMA 21 and 22, with both coastal and offshore observations taken.

OPTOMA 21 was conducted from 7 through 20 July, 1986. A primary purpose of this cruise was to make a quasi-synoptic CTD/XBT (conductivity-temperature-depth/expendable-bathythermograph) mapping of the synoptic/mesoscale variability in the NOCAL domain, placing special emphasis on the cool anomaly, meandering jet and eddy system that was present. Another purpose of the cruise was to carry out a multidisciplinary study of this eddy, jet and cool anomaly system (Mooers *et al.*, 1987; Mooers and Rienecker, 1987; Jones *et al.*, 1986; Stanton and Washburn, 1986; Washburn and Stanton, 1986; Flegal 1986; Bucklin, 1986). There was a total of 72 CTD casts and 122 XBT drops. The domain was about 150 x 250 km (Figure 2.1). The cruise consisted of a series of zig-zags, crossing a cool anomaly (see Figures 2.1 and 2.2) and then a leg into the jet near the completion of the cruise.

OPTOMA 22 was conducted 27 July through 5 August, 1986, one week following the OPTOMA 21 cruise. Besides surveying the NOCAL domain off Point Arena, California, a specific purpose of the cruise was to help define how the cool anomaly/jet system tracked in OPTOMA 21 related to a larger-scale pattern. The cruise track, shown in Figure 2.3, sampled a domain approximately 240 km square centered about 280 km off the coast between Point Arena and Cape Mendocino. 177 XBT's were successfully dropped but due to winds and high seas only six CTD casts were made. The sea surface temperature (SST) field from OPTOMA 22 was oriented along the coast (Figure 2.4). A comparison of Figure 2.4 with Figure 2.2 shows that there is a noticeable change in the orientation of the SST fields.

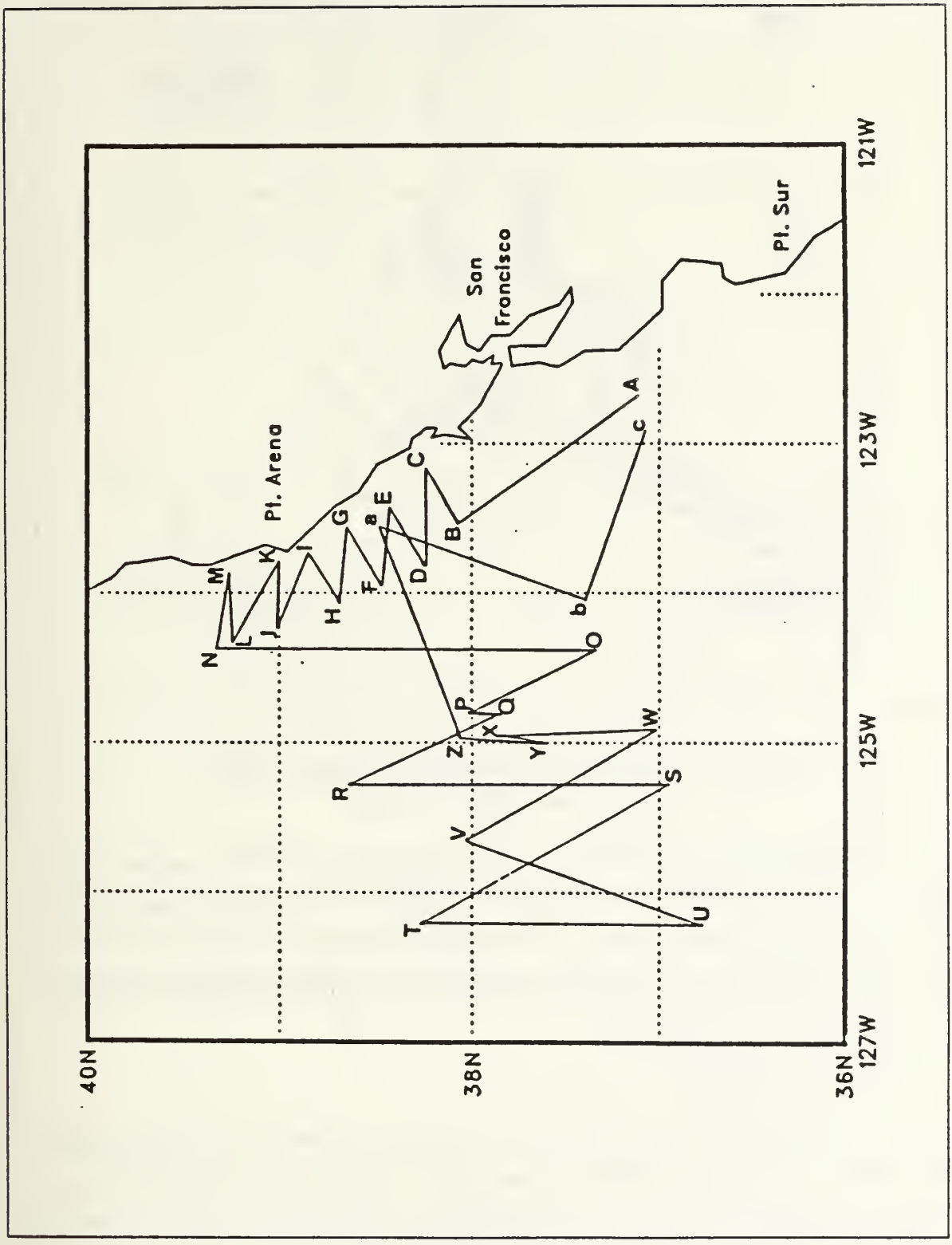

Figure 2.1 Ship track for OPTOMA 21
from Wittmann *et al.*, 1987.

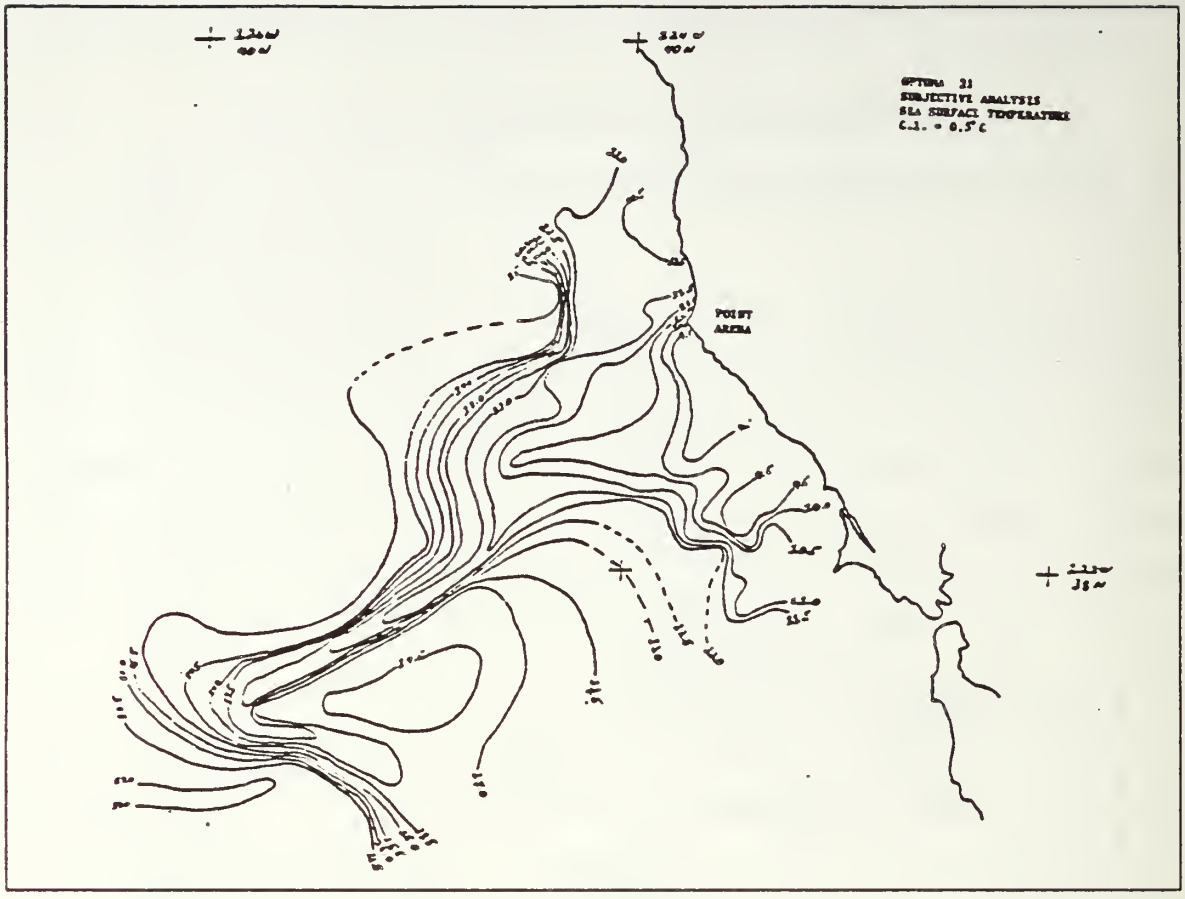

Figure 2.2 OPTOMA 21 sea surface temperature field.
The contour interval is 0.5°C.

The hydrographic data acquired from these two OPTOMA cruises will be utilized in running the objective analysis program (see section II. B) to obtain dynamic height and geostrophic current plots. For obtaining these plots, it is assumed that the data are quasi-synoptic (i.e., the dynamic structure was assumed to have not changed much over the period of sampling).

2. **Other Data Acquired**

a. Satellite Imagery

To provide real-time analysis and depiction of the jet and its movement, satellite images from Scripps Satellite Oceanography Facility (SSOF) were transmitted as soon as they were received to the ship through WWD, the radio station located at Scripps, via the facsimile (FAX). The infrared (IR) images used were advanced very high resolution radiometer (AVHRR) images from the NOAA-9 satellite. In contrast,

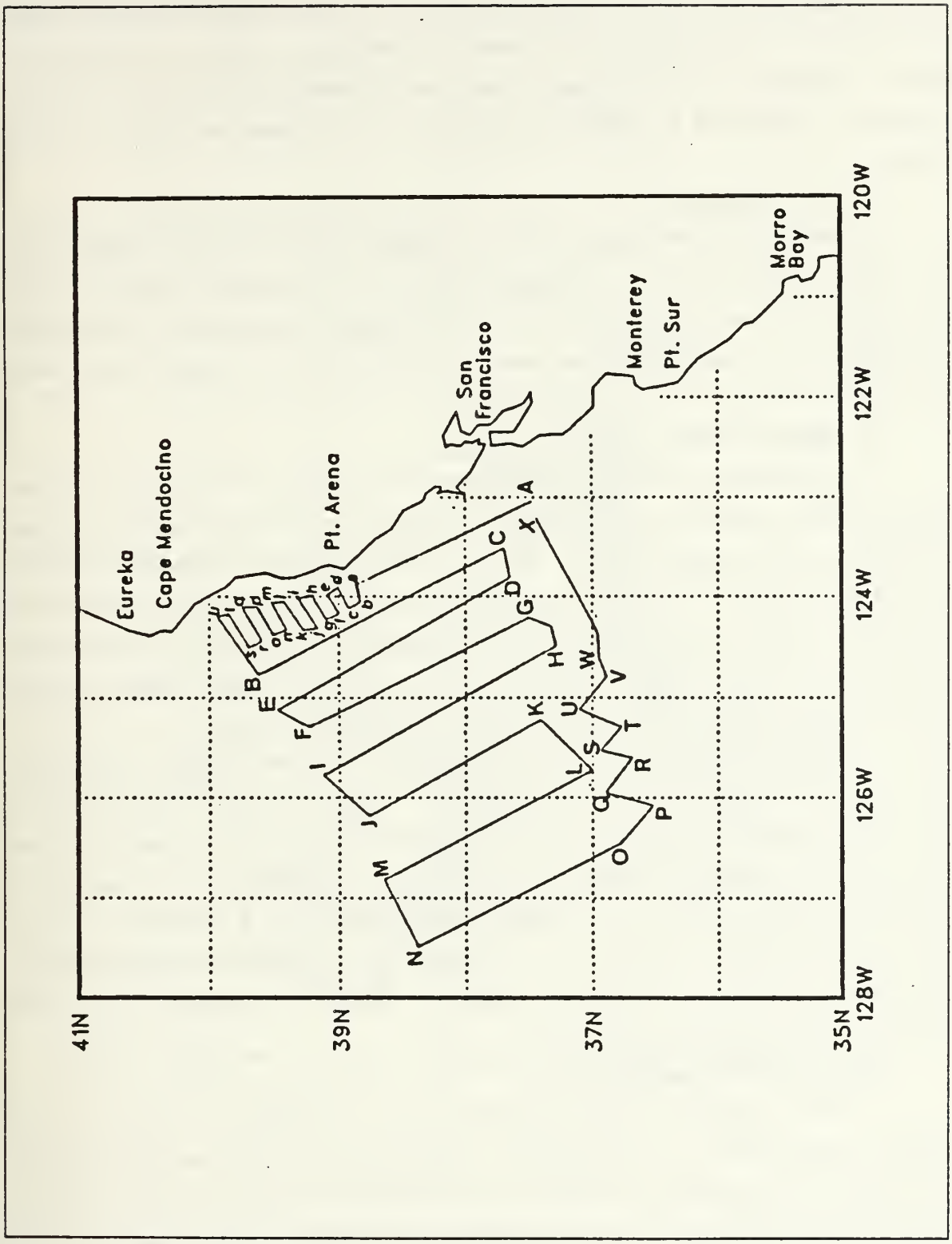

Figure 2.3 Ship track for OPTOMA 22
from Ciandro *et al.*, 1986.

IR images collected at SSOF during OPTOMA 22 were not sent directly to the ship since the ship was remapping the domain systematically instead of tracking the offshore flowing jet. These IR images, together with others from the NOAA-9 satellite, are used in Chapter III to show SST features in the CCS such as squirts, jets and meanders.

b. Buoy Wind Data

Wind data for the buoy NDBC 14, located at 39.2°N 124°W (Figure 2.5), were obtained from the National Weather Service in San Francisco, California. The data are recorded every hour and include wind direction and speed, wave information, air temperature and atmospheric pressure. A wind stick plot was made for the buoy time series at three hour intervals (Figure 2.6).

c. Bakun Upwelling Index

The Bakun upwelling indices (Bakun, 1973; Bakun, 1975; Bakun, 1986) are offshore Ekman transports computed from daily means of six-hourly synoptic surface atmospheric pressure fields from the Navy's Fleet Numerical Oceanography Center (FNOC) arranged on a 3° mesh length grid. To use this index, Bakun assumes that the offshore surface Ekman transport by the longshore component of the wind stress occurs on large enough spatial scales that it cannot be readily replaced by alongshore surface flow, but must be replaced by the upwelling of deeper waters.

The Bakun Upwelling Index to be used in the data analysis is located at 39°N, 124°W and is ~100 km to the west of the buoy NDBC 14. The proximity of this location to NDBC 14 should allow a fairly close comparison of correlations of the buoy wind and upwelling index data to be made for the immediate area. In particular, by referring to the time series plot of the upwelling index (Figure 2.7) and comparing it with the wind stickplot (Figure 2.6), a wind relaxation or reversal and the associated cessation of upwelling may be inferred. Figure 2.7 shows the upwelling index for the period 1 March through 28 August, 1986.

d. Synoptic Meteorology Charts

North American Meteorology charts for the OPTOMA 21 and 22 cruise periods, obtained from the Meteorology Department at the Naval Postgraduate School, show the large-scale wind field for North America. These charts can be used to indicate if conditions are favorable for upwelling or for wind reversals/relaxations. By combining these synoptic charts with the stickplot data and the Bakun upwelling index, winds favorable for upwelling and relaxations/reversals can be readily identified for a broader picture of the wind field.

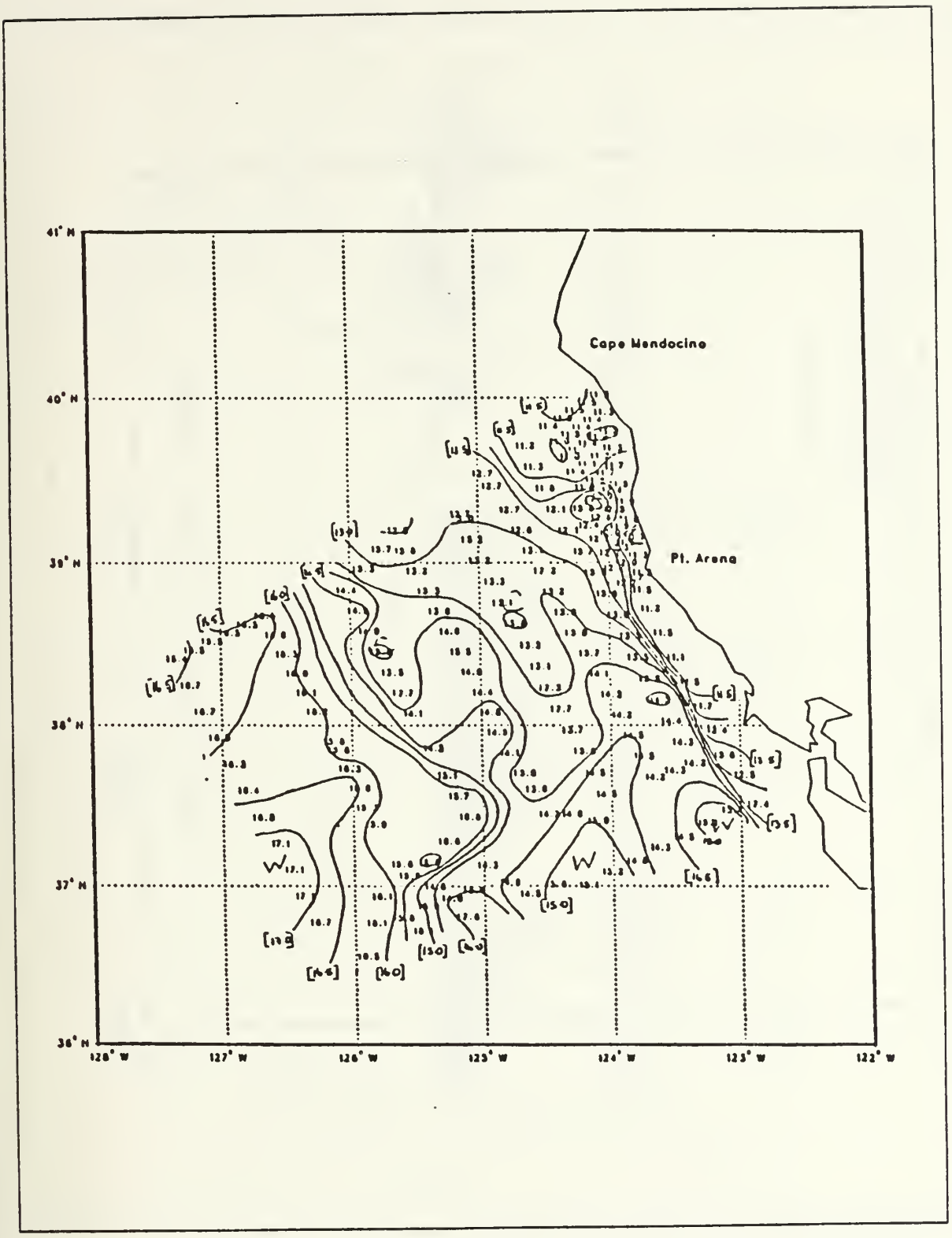

Figure 2.4 OPTOMA 22 Sea surface temperature field.
The contour interval is 0.5°C.

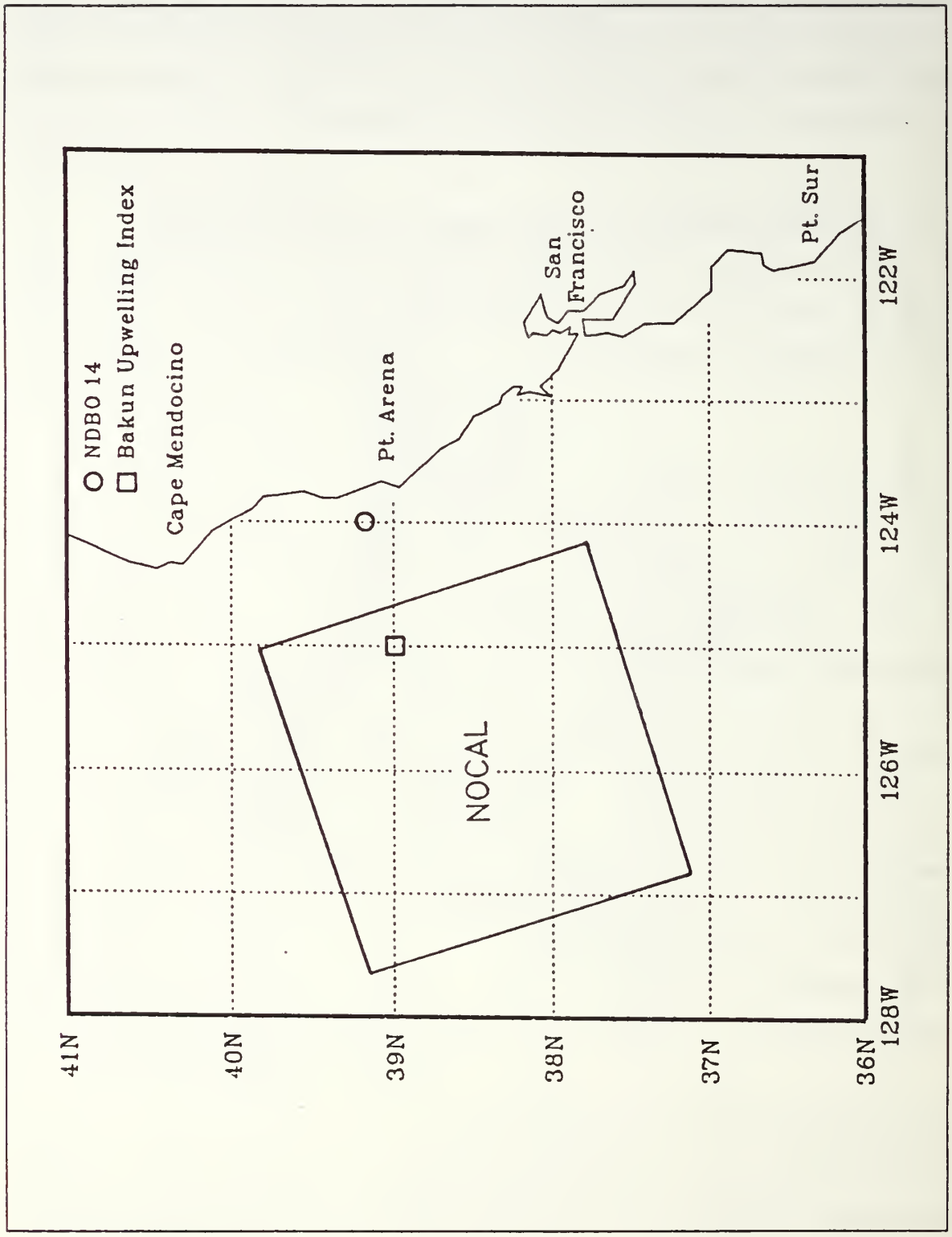

Figure 2.5 Relative positions of NDBC 14 (shown by the circle) and of the Bakun upwelling index (shown by the square).

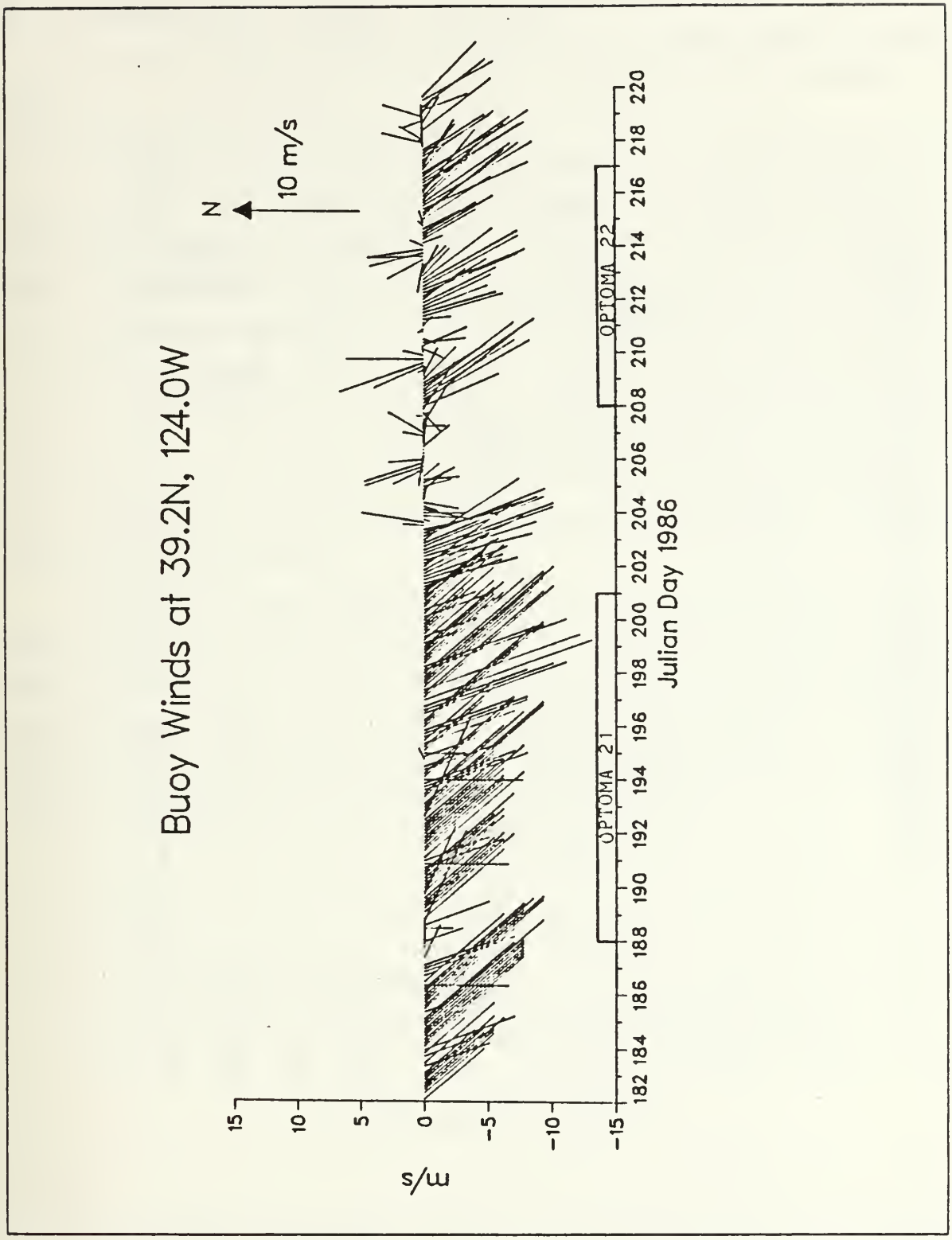

Figure 2.6 Buoy winds at 39.2°N, 124.0°W during the OPTOMA cruises.

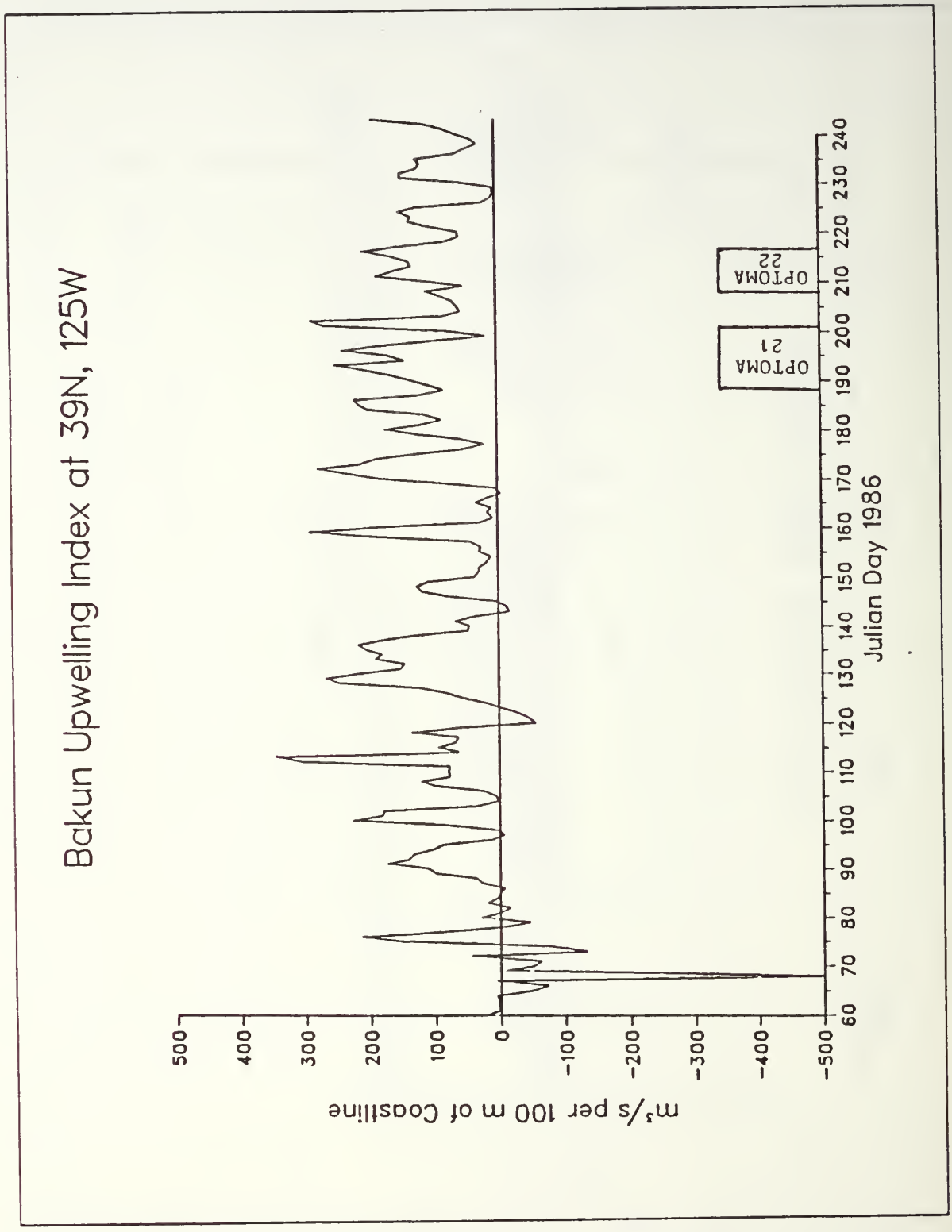

Figure 2.7 The Bakun Upwelling Index for the period 1 March through 28 August, 1986.

B. THE OBJECTIVE ANALYSIS TECHNIQUE

The objective analysis technique was first developed by Gandin (1965), applied to oceanic data by Bretherton *et al.* (1976); the program used in OPTOMA is documented by Carter and Robinson (1981).

The objective analysis program incorporates data that is irregular in time and/or space, and interpolates it objectively onto a regularly spaced grid. To do this, a correlation function must be defined. Carter and Robinson (1981) identified four specific parameters to determine the selection of observational data affecting an interpolation point. These parameters are: 1) a maximum temporal increment between observations, 2) a spatial radius of influential points, 3) a dominant phase speed, and 4) a maximum number of surrounding influential points. Obviously, it is best to use observational data closest to the interpolation point. By specifying a maximum range at which observational data may affect the interpolation point, usually determined by running a covariance program on the data, the problem of distant points influencing the interpolation can be solved.

The objective analysis program used the hydrographic data acquired by the two OPTOMA cruises to produce dynamic height and geostrophic current charts at six depth levels: 0 m, 50 m, 100 m, 150 m, 200 m, and 250 m. The dynamic heights at all levels were referenced to 450 m, a typical OPTOMA reference depth. For XBT data, the program uses a mean salinity-temperature relationship for the region. Rienecker, *et al.* (1985) estimate an rms error of 4 dyn-cm for this technique.

III. RESULTS

A. SATELLITE IMAGERY

The IR image of 18 June, 1986 (Figure 3.1), well before either cruise, indicates the complex structure of the coastal waters south of Point Arena. At the southern edge of the image a southwest oriented jet is seen, as well as what appears to be cold, newly upwelled water along the coast between Point Arena and Point Reyes.

The IR images from 14, 16 and 17 July (Figures 3.2 – 3.4) reveal the jet that was tracked by the OPTOMA 21 cruise, conducted 7 - 20 July, 1986. The jet is located just south of Point Arena, with a southwestward orientation. The first three images show the jet advecting the cold upwelled water well out from the coast, with the jet boundaries being fairly well defined. Figure 2.2, the SST plot based on data for the whole cruise, reveals the same cool anomaly seen in the IR images. This cool anomaly is associated with the offshore flowing jet tracked by the OPTOMA 21 cruise.

Following the 17 July image, cloud cover obscured the area for over a week so that the next good image of the area obtained was on 29 July (Figure 3.5). This was the first day of the OPTOMA 22 cruise. Although the coastal waters were obscured by low clouds or fog, it is apparent that the flow field has changed. No longer are offshore filaments or jets visible. Instead, a field of mixed water with the general flow parallel instead of perpendicular to the coast is seen. The next clear image was on 30 July (Figure 3.6). A band of clouds stretches from Point Reyes southwest, partially obscuring the flow field. Again though, the flow field is oriented along the coast instead of being perpendicular to the coast as seen in the earlier images (i.e., Figures 3.2 – 3.4). Also noted is the warm water adjacent to the coast south of Point Arena. No other images were obtained due to cloudy, overcast conditions until well after the OPTOMA 22 cruise had ended on 5 August.

B. WIND DATA

As can be seen in the velocity time series, commonly referred to as a stickplot diagram (Figure 2.6), the winds in the region are equatorward, or favorable for upwelling, throughout the OPTOMA 21 cruise. However, by July 22 (Julian day 203) a low pressure system had moved into the area off the California Coast. The cyclonic flow of this system reversed the winds so that they blew poleward instead of

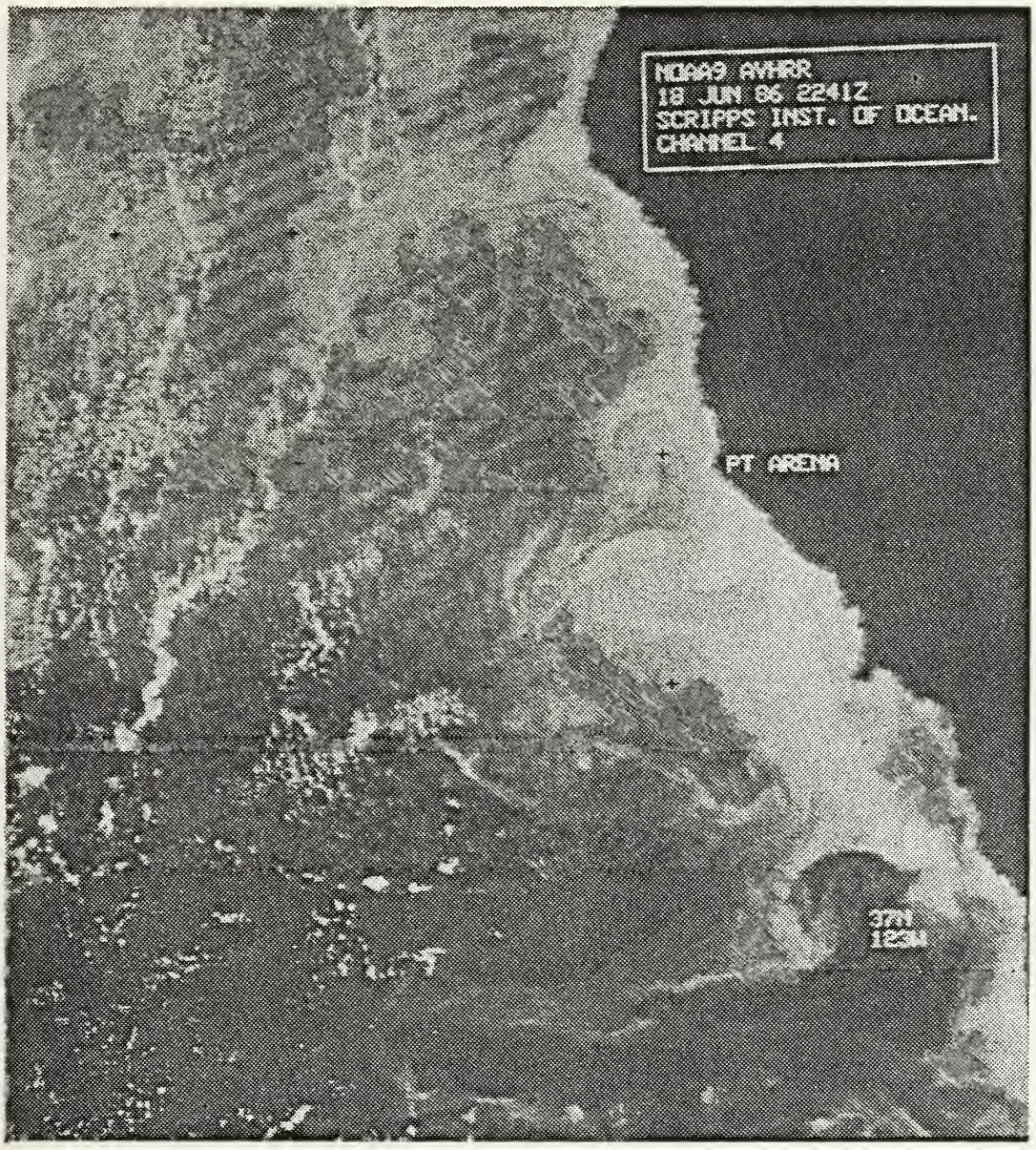

Figure 3.1 NOAA-9 satellite IR image, 18 June, 1986.

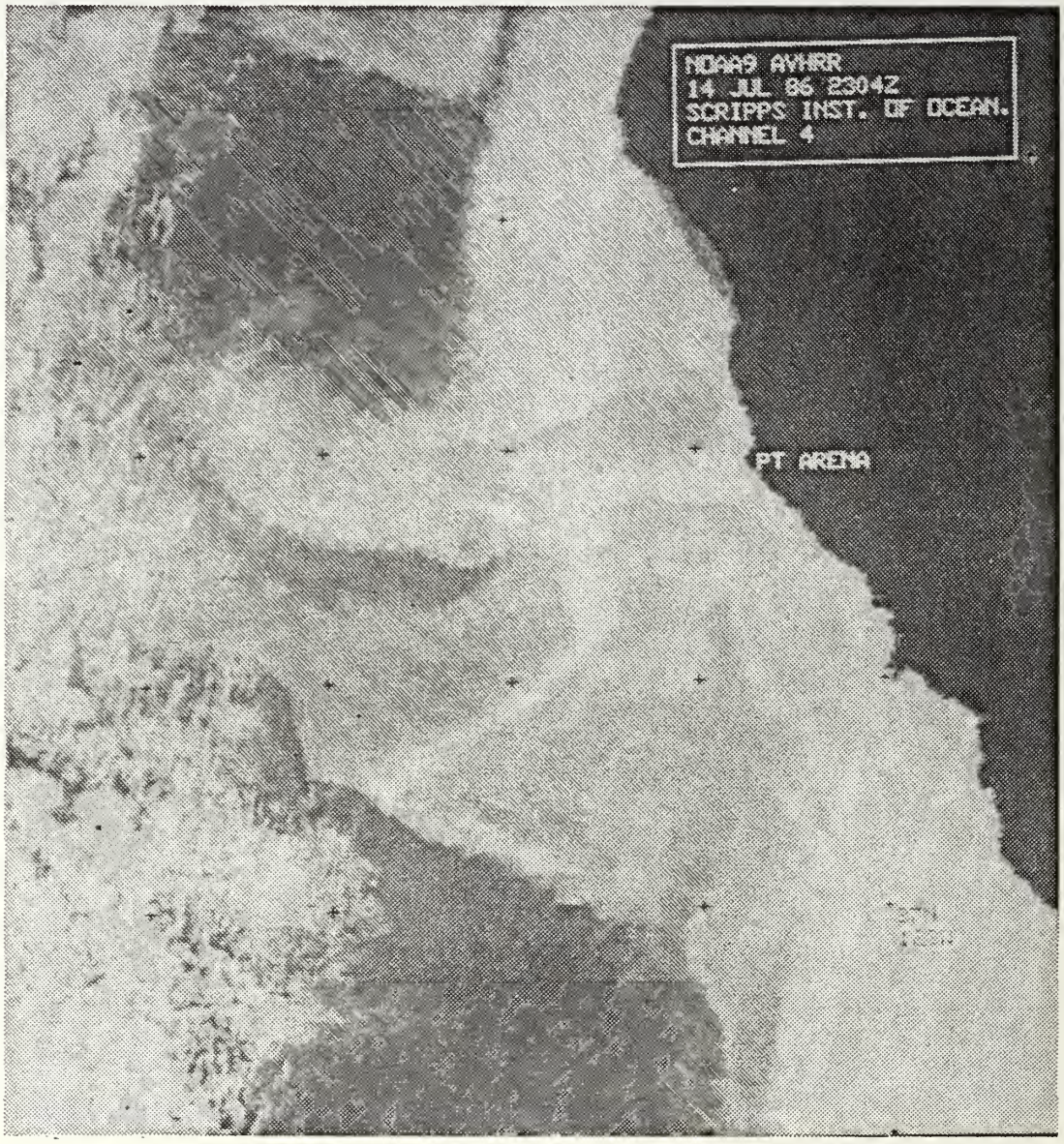

Figure 3.2 NOAA-9 satellite IR image, 14 July, 1986.

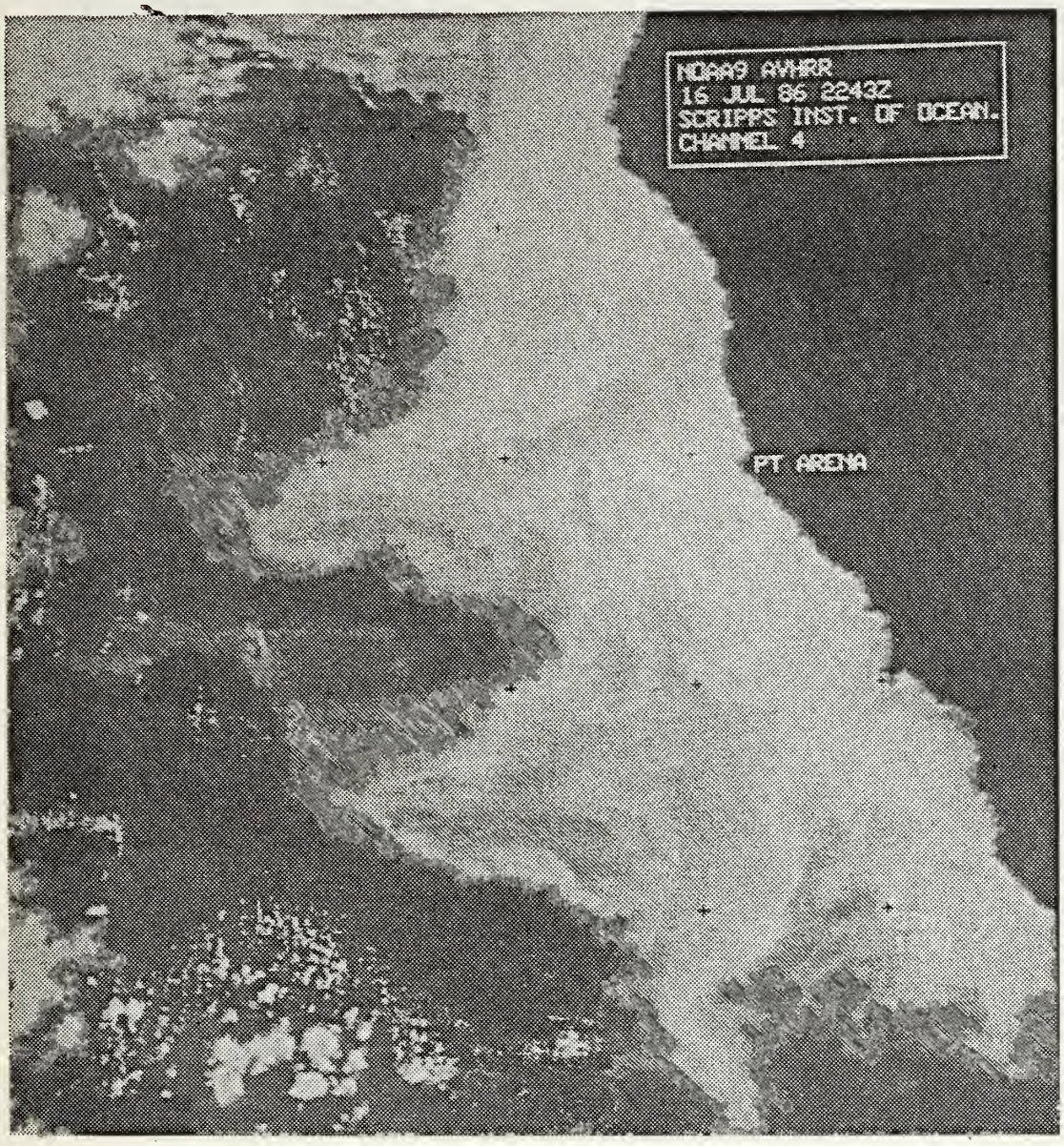

Figure 3.3 NOAA-9 satellite IR image, 16 July, 1986.

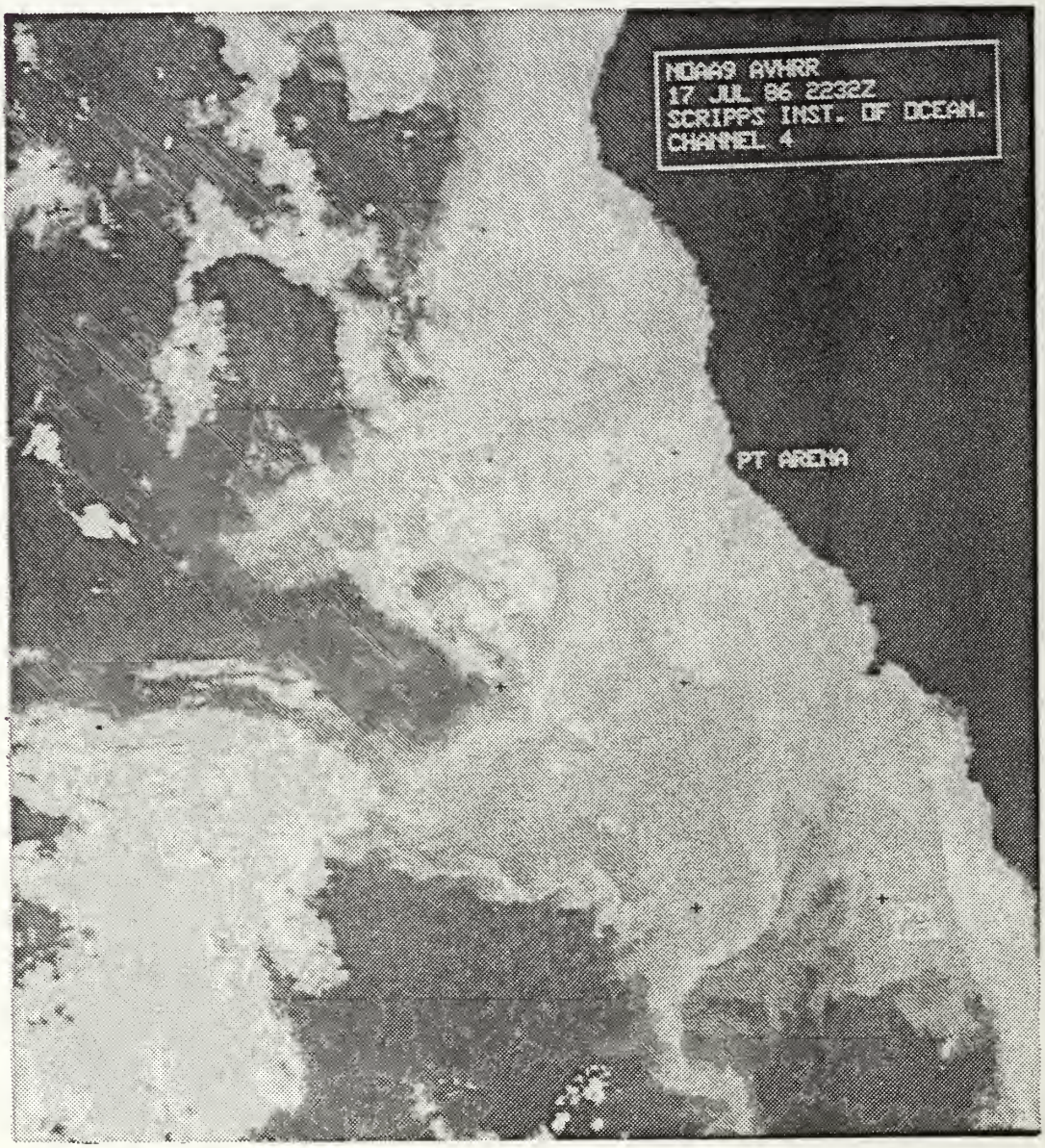

Figure 3.4 NOAA-9 satellite IR image, 17 July, 1986.

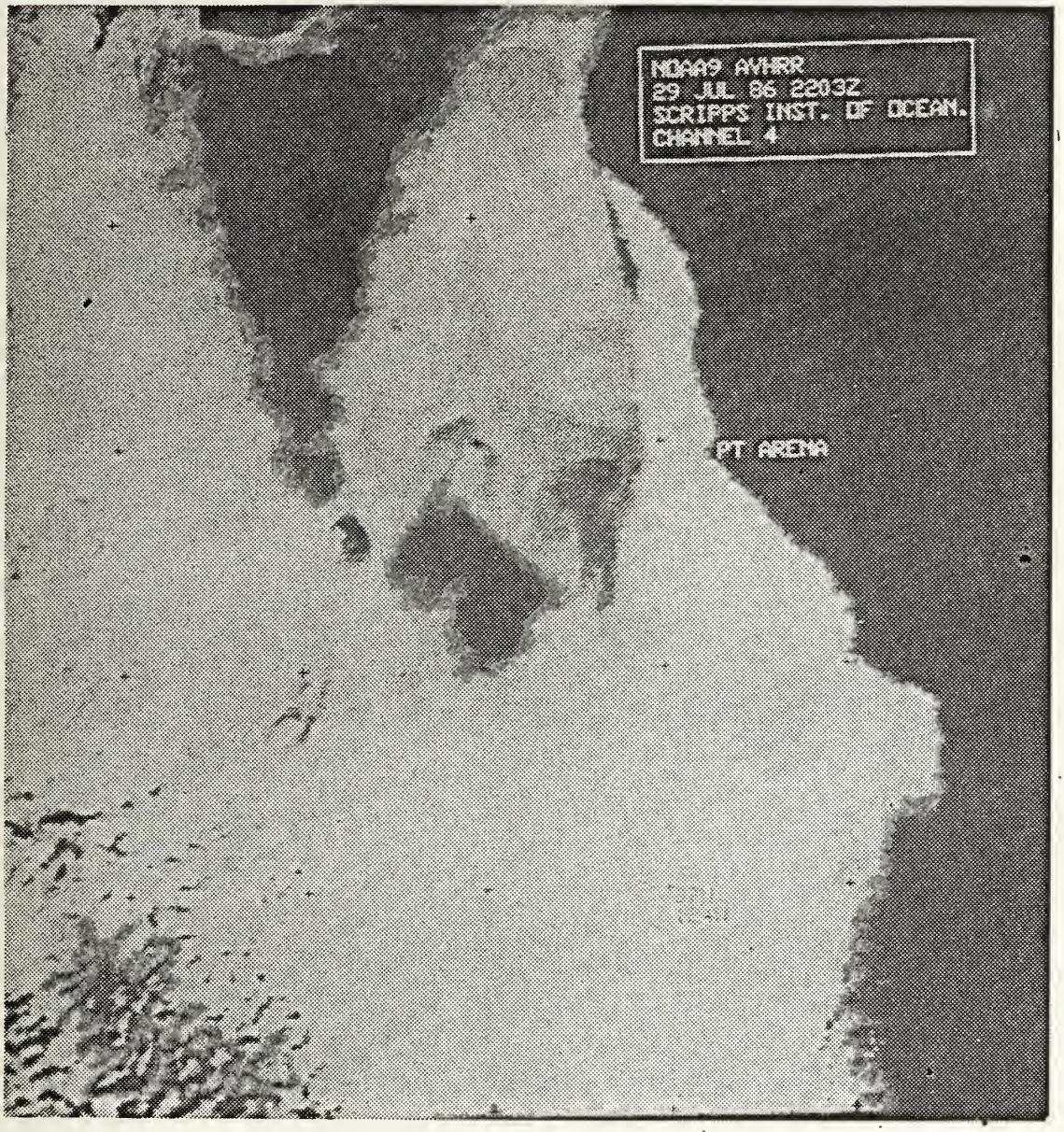

Figure 3.5 NOAA-9 satellite IR image, 29 July, 1986.

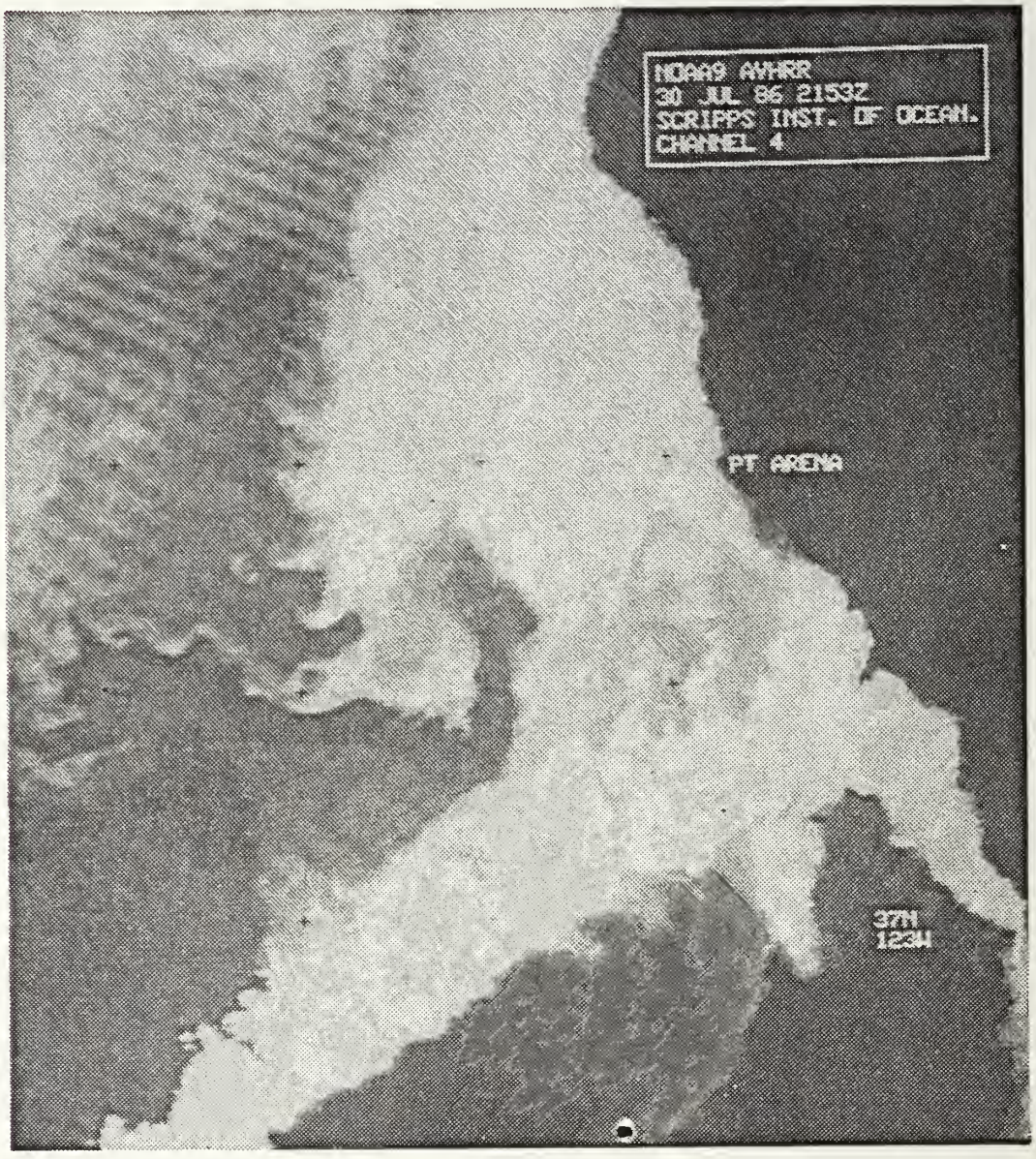

Figure 3.6 NOAA-9 satellite IR image, 30 July, 1986.

equatorward, as observed at NDBC 14 (Figure 3.7). These poleward winds continued for almost 24 hours, which disrupted the surface water circulation of offshore flow and consequently broke up the upwelling.

Comparing Figure 2.6 with the Bakun Upwelling Upwelling Index (Figure 2.7), the following correlations can be made. Following the OPTOMA 21 cruise, a decrease in the index, indicating less upwelling was occurring, is noted on Julian day 204 (July 22). As expected, there is a short time lag between the wind cessation/reversal and the dynamical ocean response. The winds are equatorward again on 23 July (Figure 2.6) in response to the 'normal' atmospheric situation with the North Pacific High and the southwestern United States thermal low (Figure 3.8).

After slightly more than 24 hours of equatorward winds, another wind reversal occurred on 24 July, Julian day 205 (Figures 2.6 and 3.9). This wind reversal followed that of 22 July close enough that the Bakun Upwelling Index (Figure 2.7) did not indicate a significant increase in upwelling between the two poleward wind events. Figure 3.10 shows the equatorward winds at the beginning of the OPTOMA 22 cruise. Again equatorward winds dominated the atmospheric regime from 26-28 July (Figure 2.6). Then, on 28 July (Julian day 209), poleward winds (Figures 3.11 and 2.6) resulted in a corresponding decrease in the Bakun Upwelling Index (Figure 2.7).

C. ANALYSIS OF HYDROGRAPHIC DATA

1. OPTOMA 21

a. Dynamic Topography and Geostrophic Current Analysis

Figures 3.12 – 3.17 show the dynamic topography and geostrophic currents of the domain, produced by the objective analysis technique, for OPTOMA 21. The plots are at 50 m depth intervals and are relative to 450 m, a typical reference level for the OPTOMA program (Rienecker *et al.*, 1985). Each dynamic topography/geostrophic current plot pair are at the same depth. The OPTOMA 21 dynamic topography at the surface (Figure 3.12 a) shows the same general water structure as that shown by the hand contour analysis of the SST (see Figure 2.2), i.e., a cold water jet extending ~200 km southwest of Point Arena. On the dynamic topography map, the center of the jet can be seen at 37.5°N, 124.8°W. This jet is most likely the result of cold water upwelled from the colder subsurface water, since the winds before and during the cruise were favorable for upwelling (Figure 2.6). Anticyclones are seen to the southwest and northwest of the topographic low.

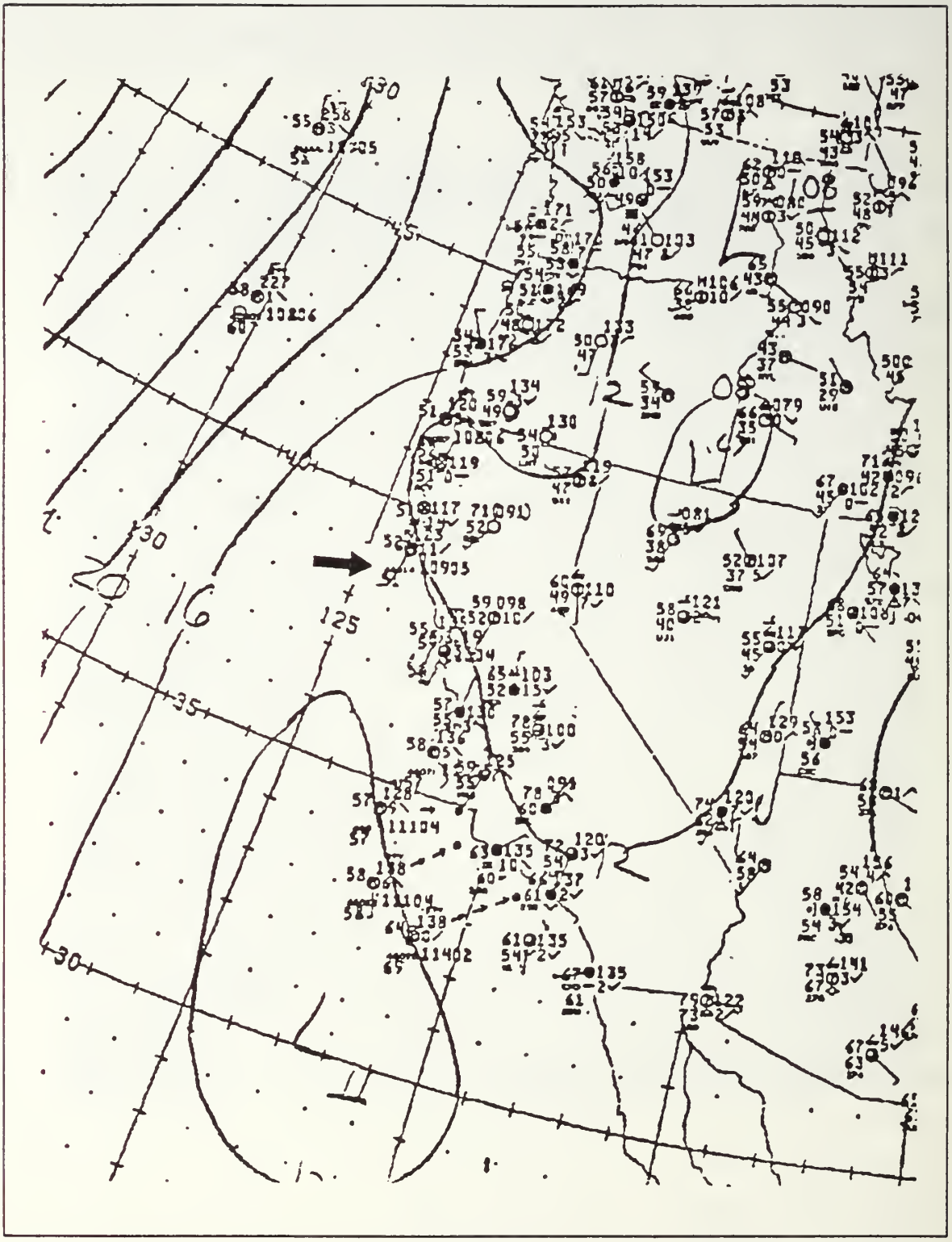

Figure 3.7 Poleward winds following the OPTOMA 21 cruise 12Z 22 July, 1986. Arrow denotes NDBC 14..

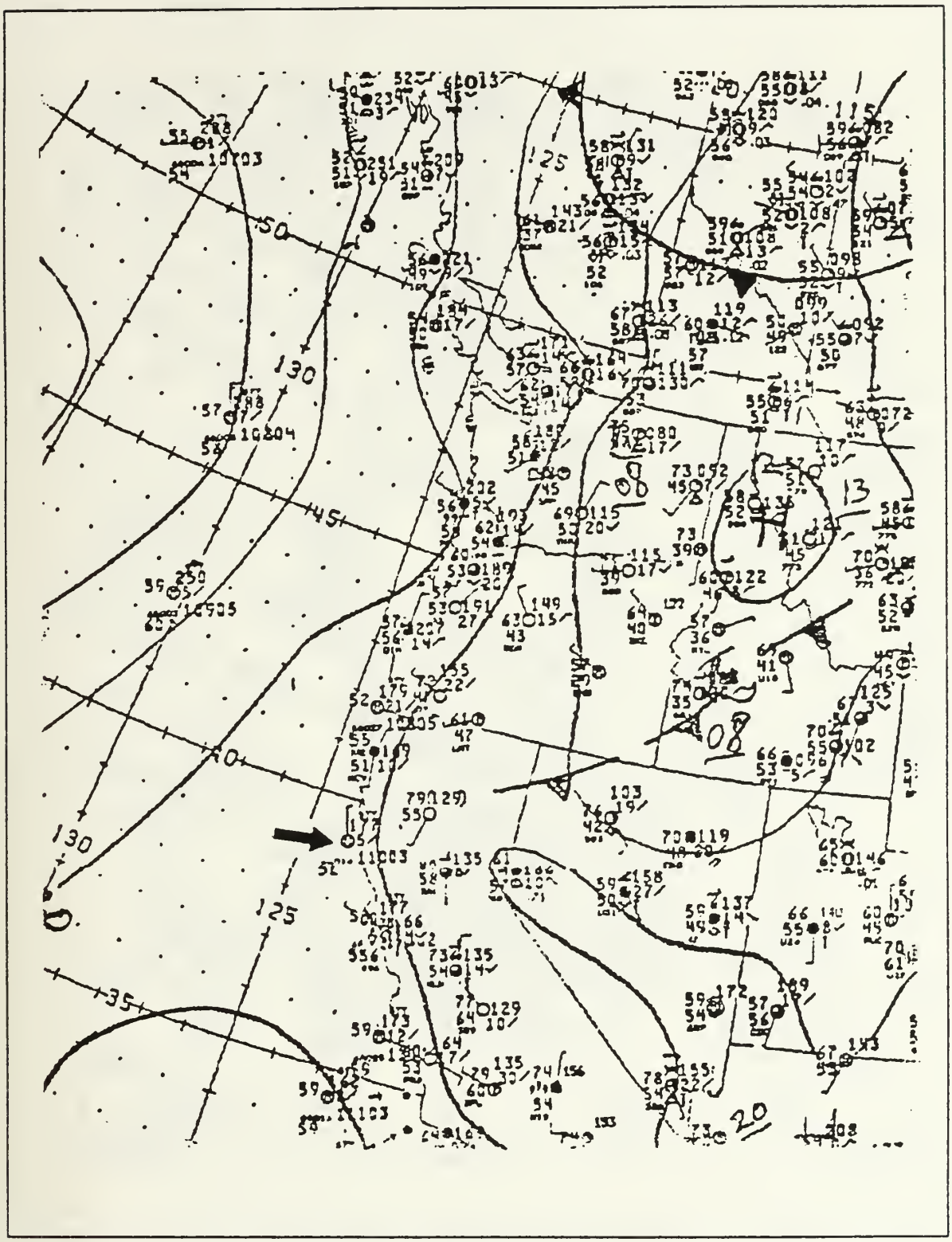

Figure 3.8 Cessation of poleward winds immediately following the OPTOMA 21 cruise, 06Z 23 July, 1986.

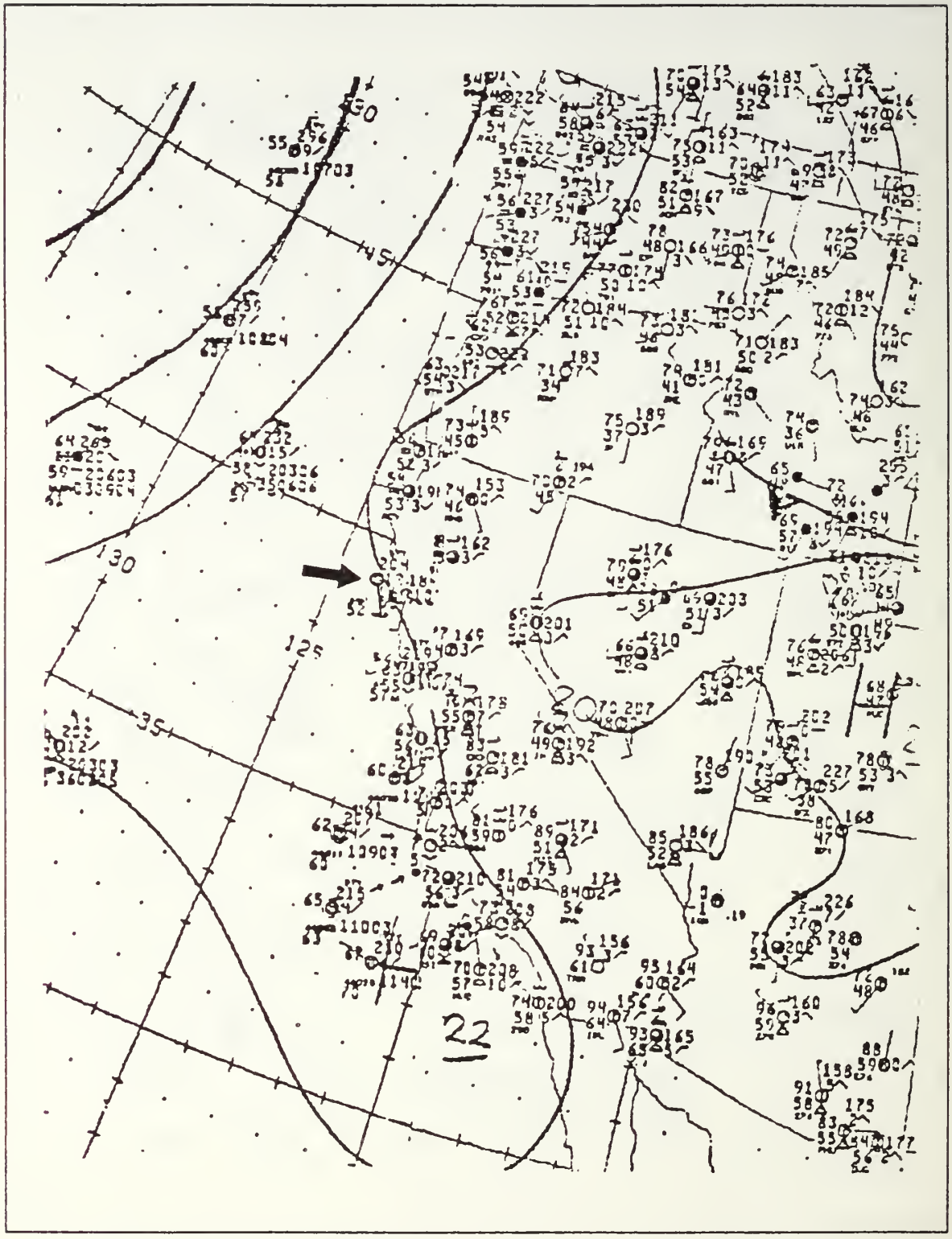

Figure 3.9 Start of poleward winds prior to OPTOMA 22 cruise
18Z 24 July, 1986.

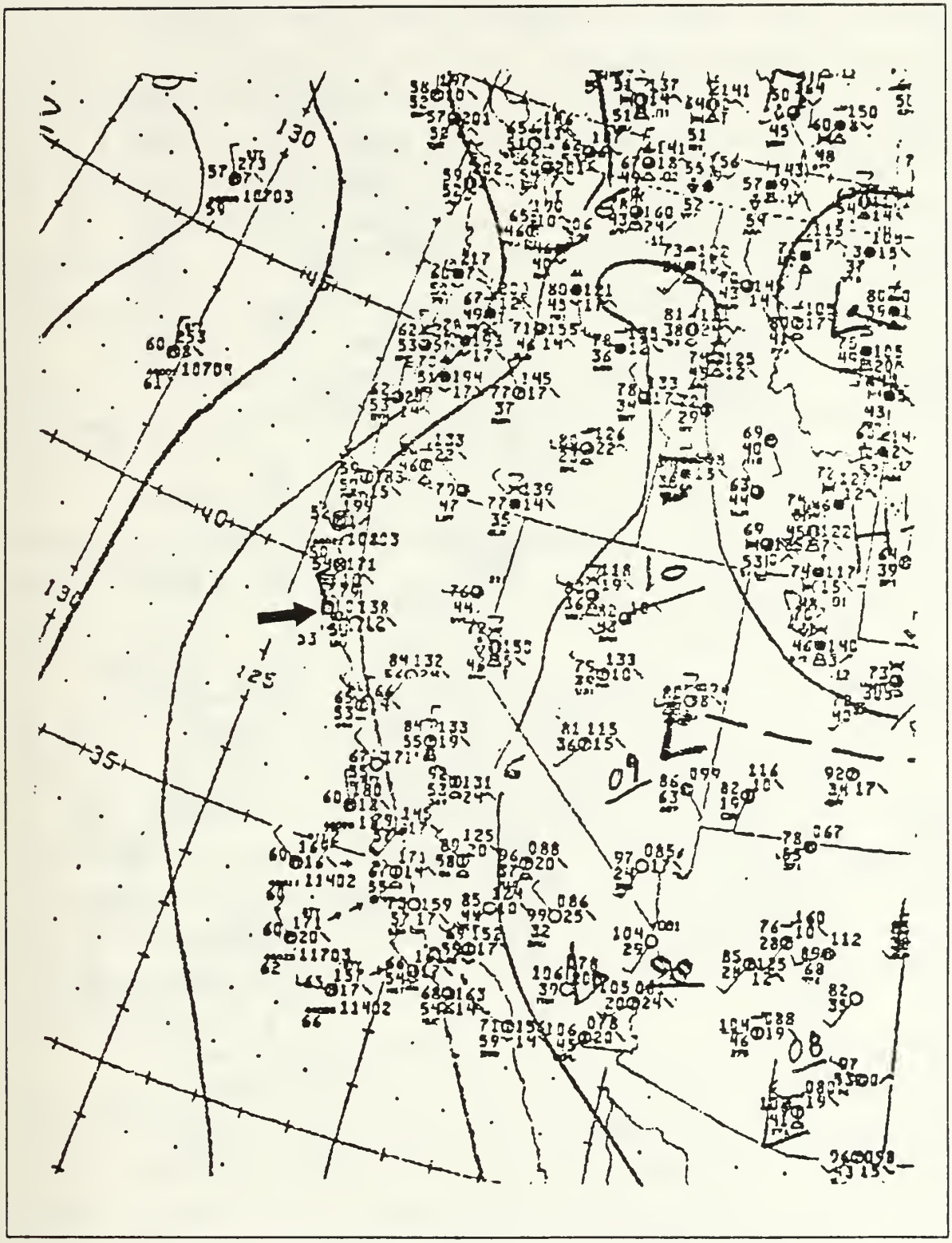

Figure 3.10 Cessation of poleward winds prior to OPTOMA 22 cruise 00Z 27 July, 1986.

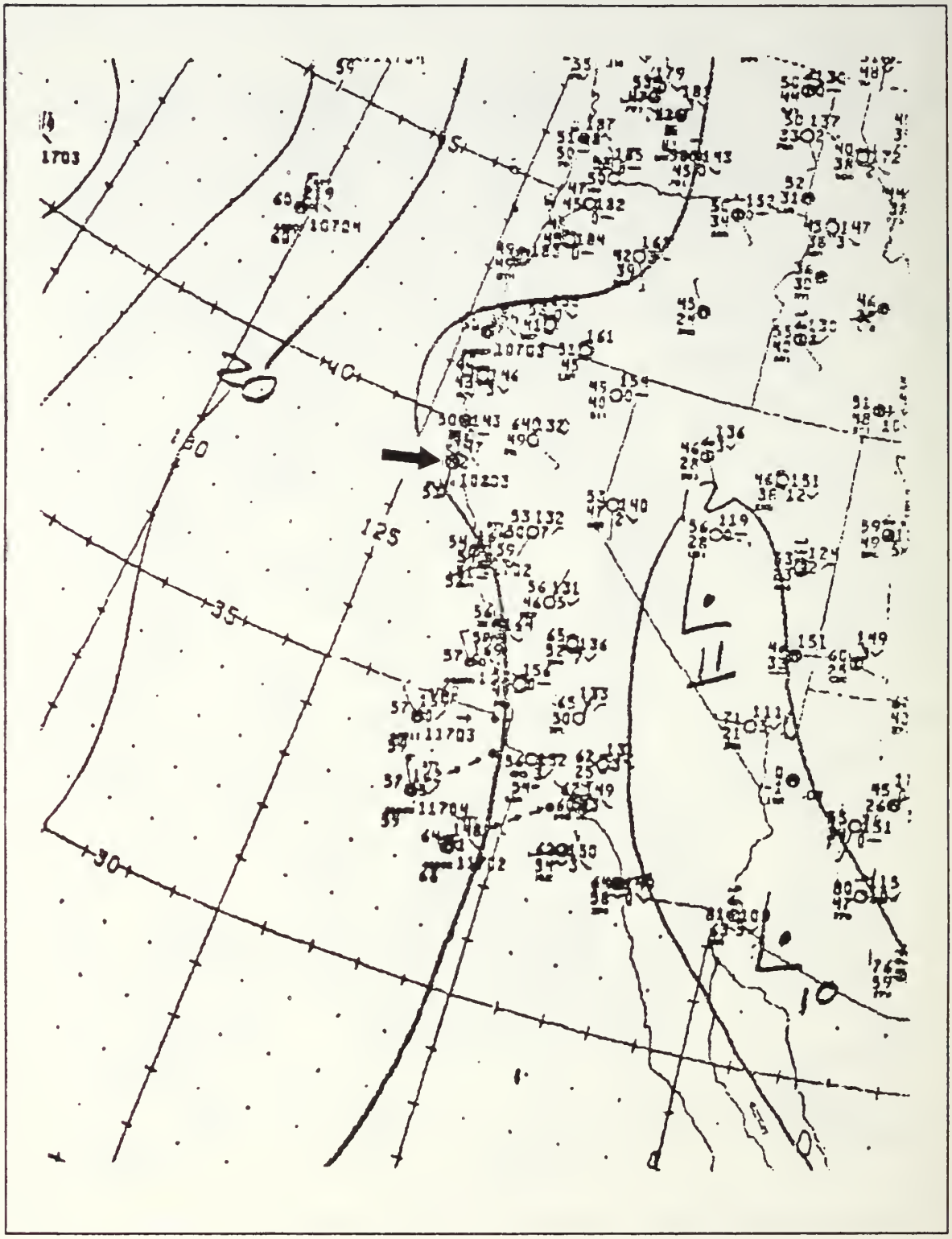

Figure 3.11 Start of poleward winds during the OPTOMA 22 cruise 12Z 28 July, 1986.

The coastal currents have a maximum of ~25 cm/s, while the offshore currents reach a maximum of ~45 cm/s. There was a general equatorward geostrophic flow, both along the coast and offshore (Figure 3.12 b). The low (Figure 3.12 a) is part of a cyclonic current. The southwestward currents to the north of this low have a maximum of ~30 cm/s.

At 50 m depth (Figure 3.13 a), the upwelled jet is still discernible. The shoreward side of the low was "pinched". The anticyclones appear to have moved slightly to the east, now being oriented further north and south of the low.

The geostrophic currents (Figure 3.13 b) at this depth exhibit the same general flow characteristics and strengths as at the surface. However, the westward flow to the north of the low is less than at the surface, with maximum currents on the order of ~25 cm/s.

At the 100 m depth (Figure 3.14 a) the 'pinching' of the upwelled jet is evident, with the low now represented by closed contours. This is accentuated by an anticyclonic eddy discernible near the eastward extent of the anticyclone southwest of the low, just west of San Francisco Bay. This is the deepest level that evidence of the jet can be seen.

The geostrophic currents for this depth (Figure 3.14 b) are still generally southward. The currents are however, weaker with maxima of ~10 cm/s near the coast and ~25 cm/s in the southern portion of the main offshore flowing jet.

Eddy-like structure is revealed by the current pattern. The eddy-like structure at this and deeper depths could well be artifacts of the objective analysis technique, since the objective analysis error fields (not shown) are greatest where the eddy-like structure is seen. A smaller domain size than used here for the objective analysis program could well reduce the error fields, since they are mainly a result of sparsely sampled data.

The deeper levels, i.e., 150 m, 200 m and 250 m (Figures 3.15 a – 3.17 a), all show the intricate structure of eddies. There is no jet signature. An anticyclone is seen south of Point Arena. An anticyclone west of San Francisco Bay, first seen in the 100 m depth, is discernible. A low that was linked with the offshore jet in the upper layers is seen in the lower layers as a large cyclonic eddy. The anticyclone southwest of the low recedes to the west with depth. To the north is an anticyclonic eddy.

The geostrophic currents of the deepest three depths (Figures 3.15 b – 3.17 b) clearly indicate an eddy structure and a lack of any generalized equatorward flow.

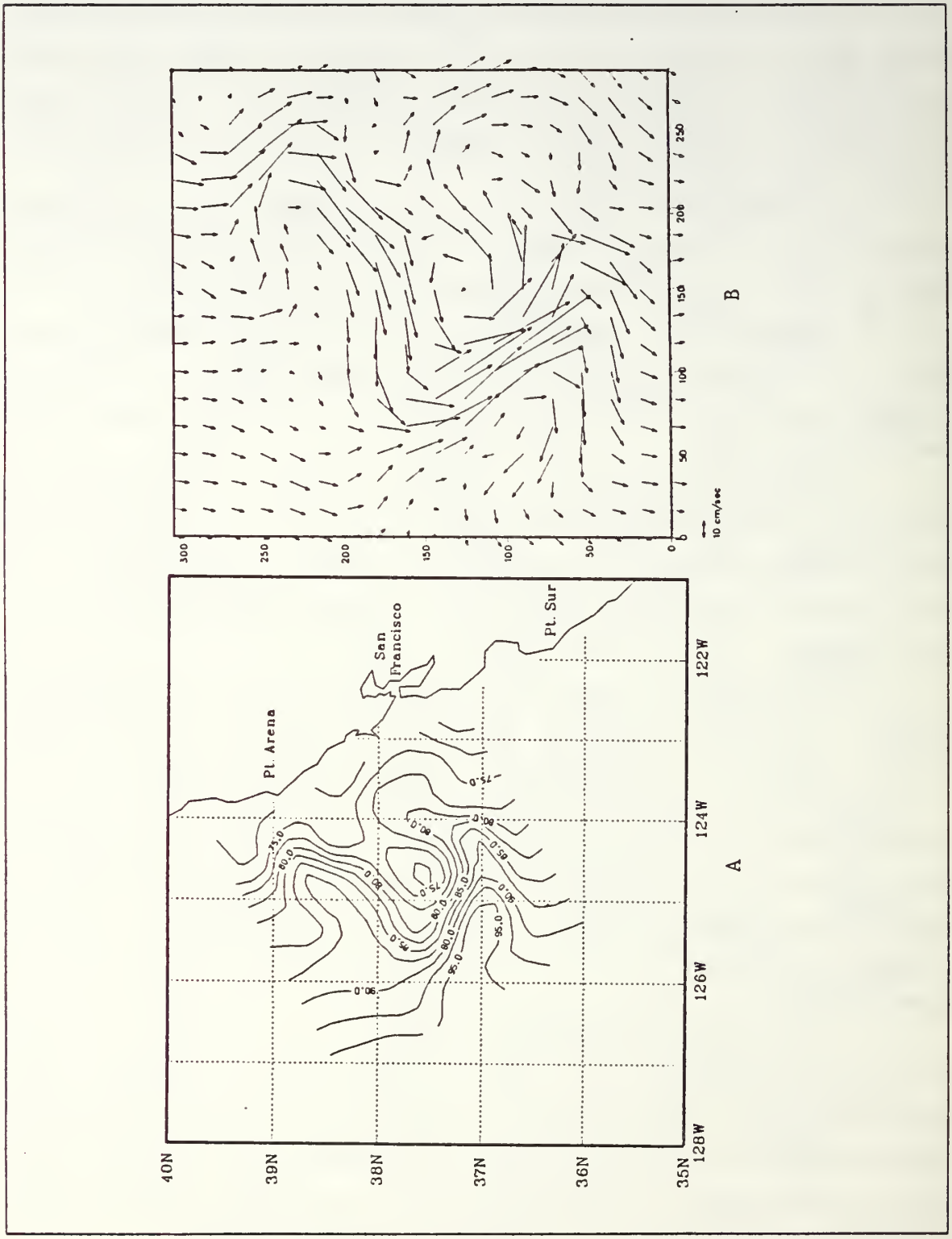

Figure 3.12 OPTOMA 21 (A) Surface dynamic topography and (B) Surface geostrophic currents.

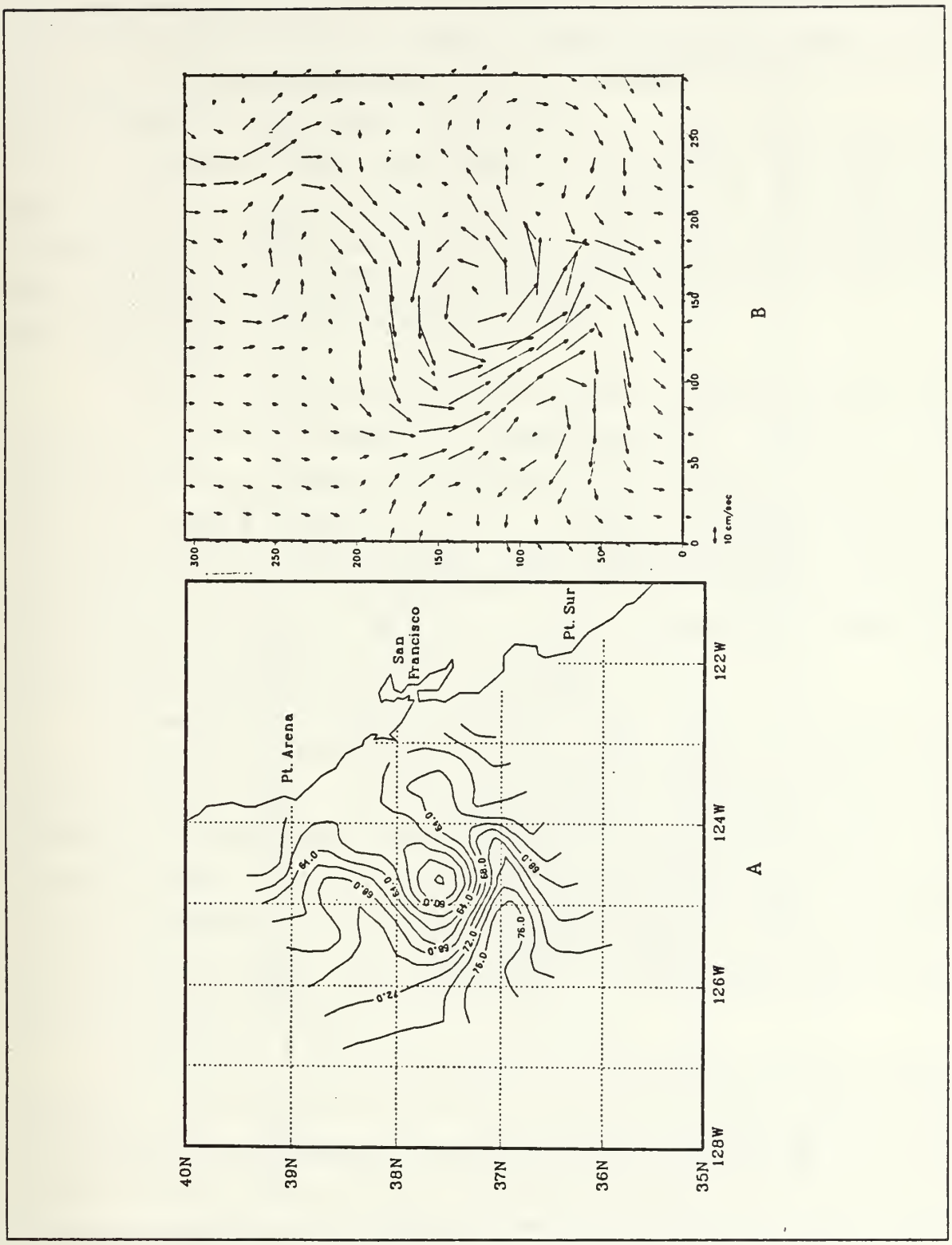

Figure 3.13 OPTOMA 21 (A) 50 m depth dynamic topography and (B) 50 m depth geostrophic currents.

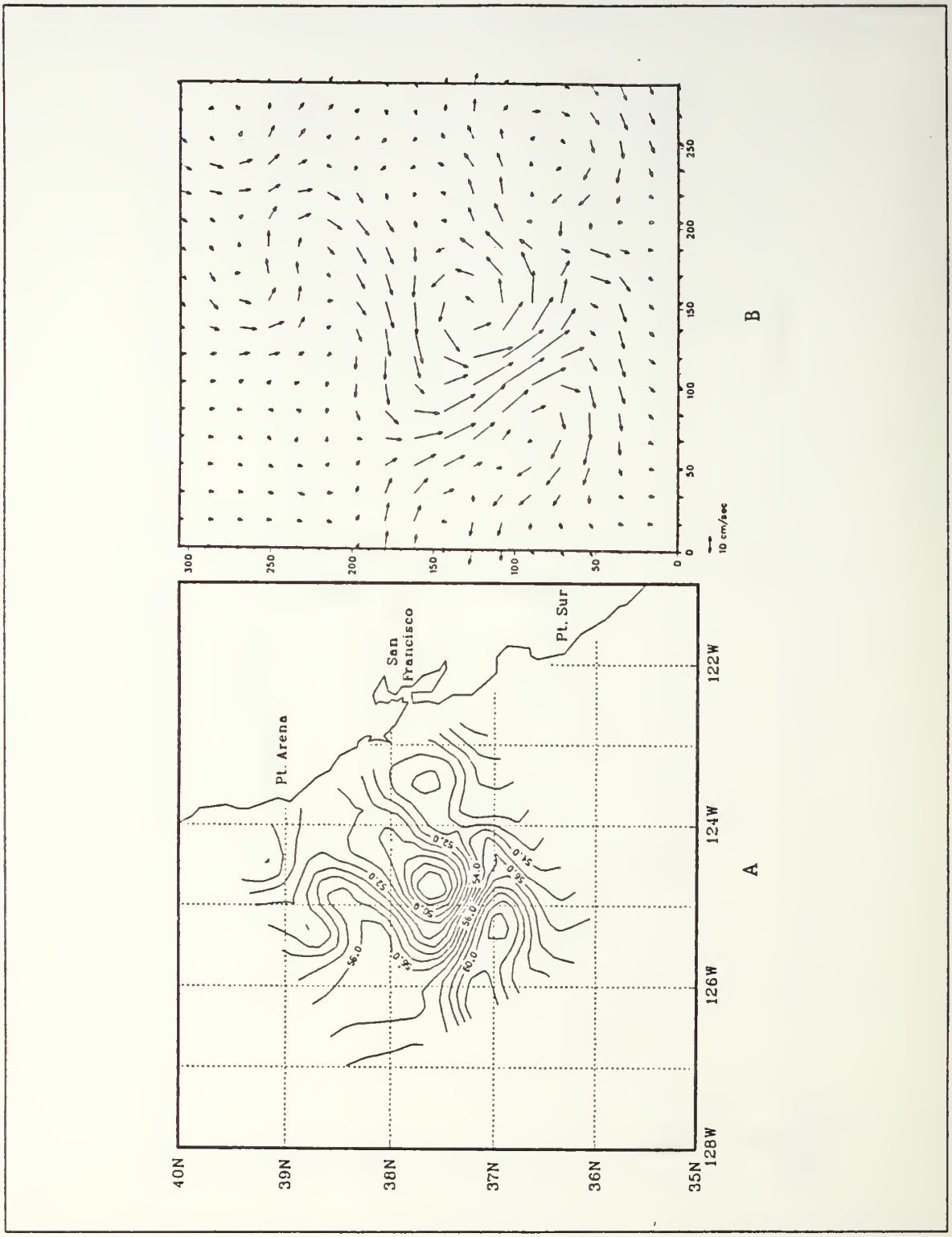

Figure 3.14 OPTOMA 21 (A) 100 m Dynamic Height Topography and (B) 100 m geostrophic currents.

The currents at these depth levels are weak, ranging from a maximum in the current field of ~15 cm/s at 150 m to a maximum of ~10 cm/s at the 250 m depth. At the 250 m depth two eddies are discernible which are cyclonic remnants of the low and the anticyclonic flow of the high off San Francisco Bay.

In general, the winds were favorable for upwelling prior to and through the OPTOMA 21 cruise. This resulted in coastal upwelling with an offshore jet 'originating' from a locally intense upwelling region. This is consistent with the same type of upwelling pattern that Kosro and Huyer (1987) found during CODE when equatorward winds were dominant (primarily in 1981).

b. T-S Diagrams

Figures 3.18 and 3.19 show the OPTOMA 21 temperature-salinity (T-S) diagrams for nearshore and offshore CTD stations, respectively. A comparison of the diagrams shows that the upper layer temperatures from the offshore CTDs can be as much as 3 K higher (i.e., maximum of ~17°C vice that of ~14°C) than those from the nearshore CTDs. The salinities span a broader range (1‰ compared to 0.5‰) for the offshore CTDs than for to the nearshore CTDs. At greater depths the same overall T-S relationship is depicted at both the nearshore and offshore CTD stations, but extend for greater depths for the offshore stations, as expected.

c. Vertical Cross Sections of the Domain

Two vertical cross sections from the OPTOMA 21 survey were drawn, one along the upwelled jet and one across the jet. These two sections are shown on the OPTOMA 21 survey station diagram, Figure 3.20. In the figure, transects are identified by letters. The cross sections were drawn from the XBT and CTD data. The sections are of temperature and salinity and are drawn to 750 m depth. The contour interval for the temperature cross section is 0.5°C for temperatures less than 10°C, and 1°C for temperatures greater than 10°C. The salinity cross section contour interval is 0.1‰ for all salinities.

The vertical cross section taken along the upwelled jet, A-B, is shown in Figure 3.21. The temperature cross section (Figure 3.21 a) reveals a broad upwelling of cool water with a general southward geostrophic flow (out of the page to the reader) down to ~250 m. Below ~200 m the isotherms are level or have a reverse tilt indicating a northward flow. However, near the coast at depths greater than ~150 m, the downward tilting of isotherms indicate warm water and a northward flow.

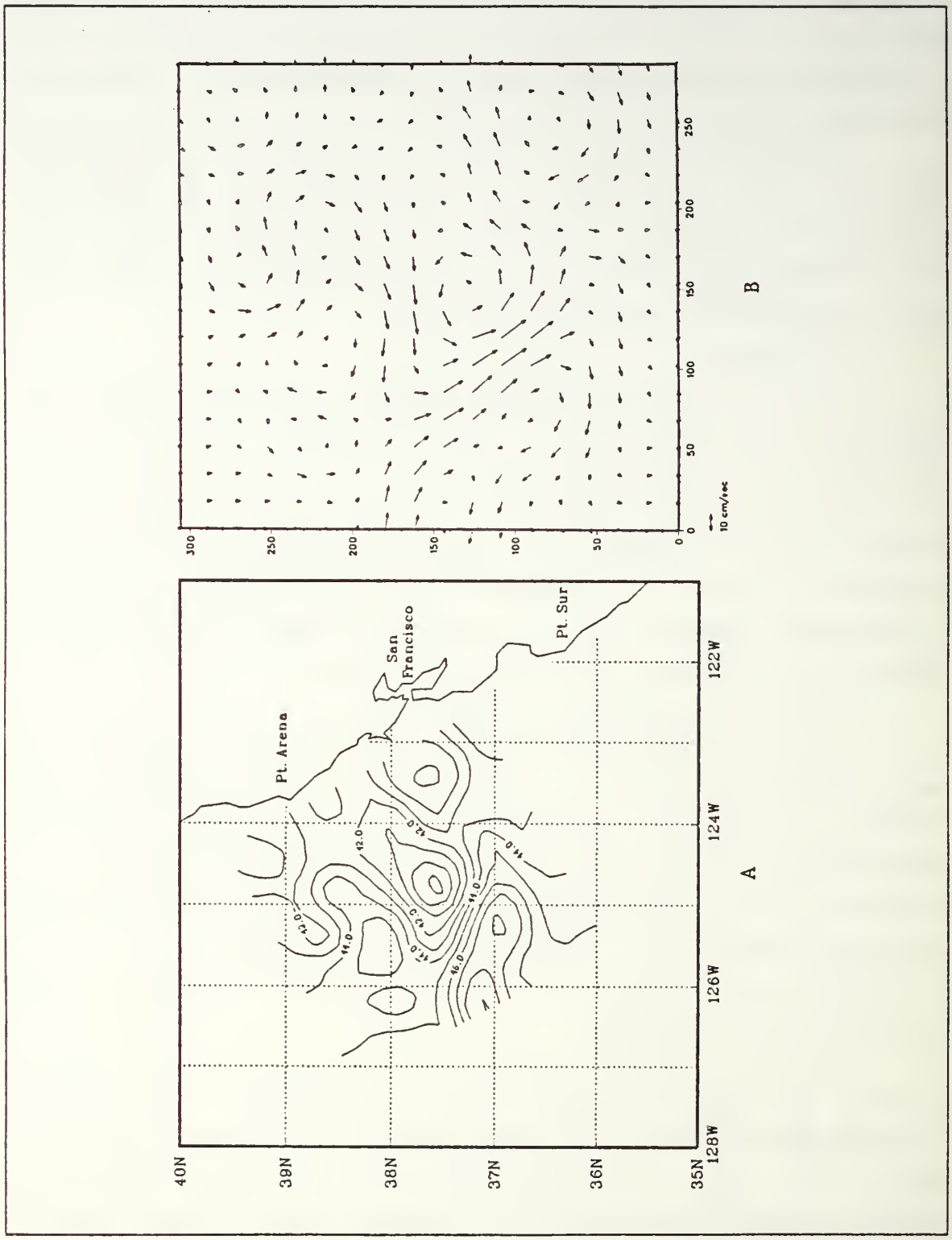

Figure 3.15 OPTOMA 21 (A) 150 m dynamic topography and (B) 150 m geostrophic currents.

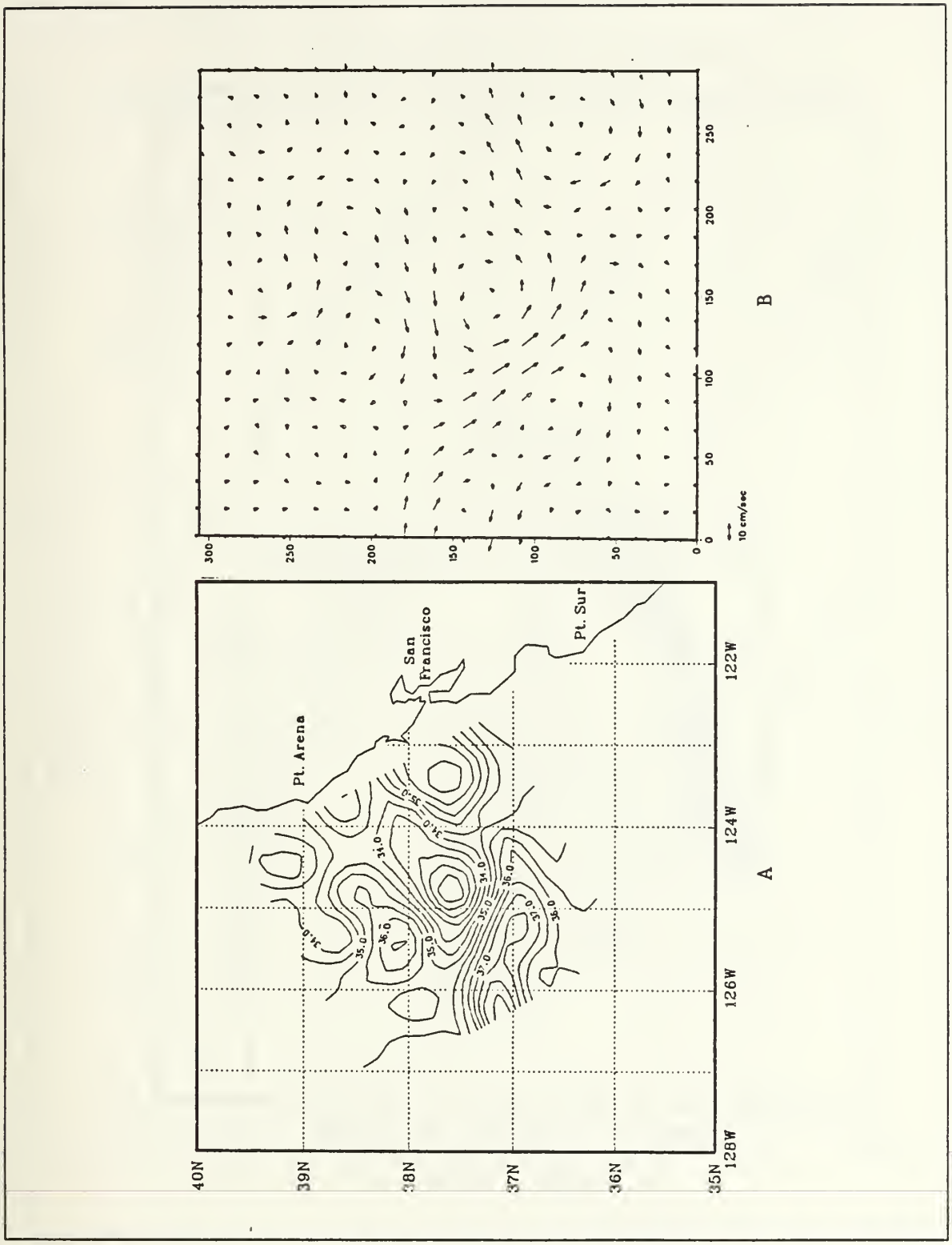

Figure 3.16 OPTOMA 21 (A) 200 m dynamic topography and (B) 200 m geostrophic currents.

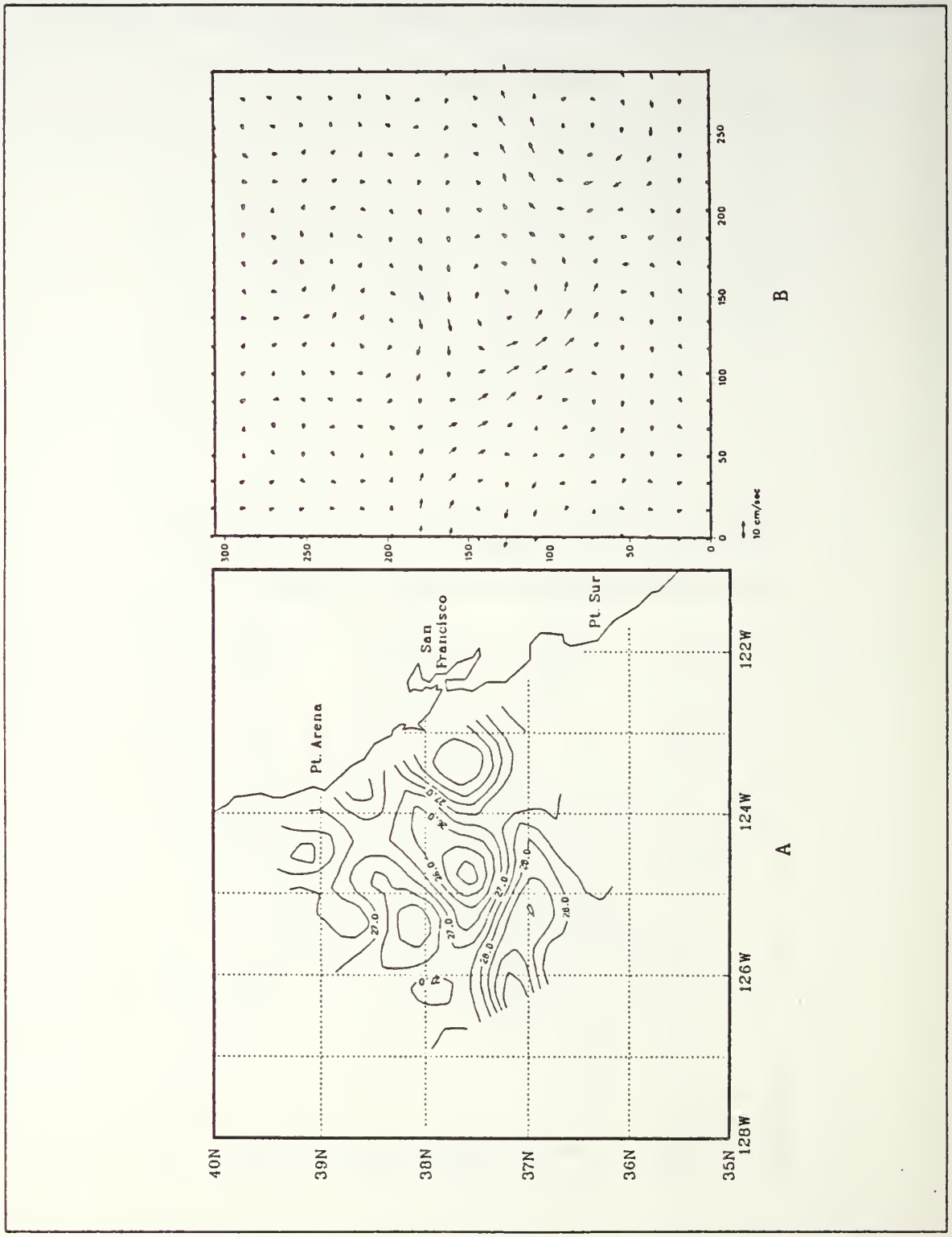

Figure 3.17 OPTOMA 21 (A) 250 m dynamic topography and (B) 250 m geostrophic currents.

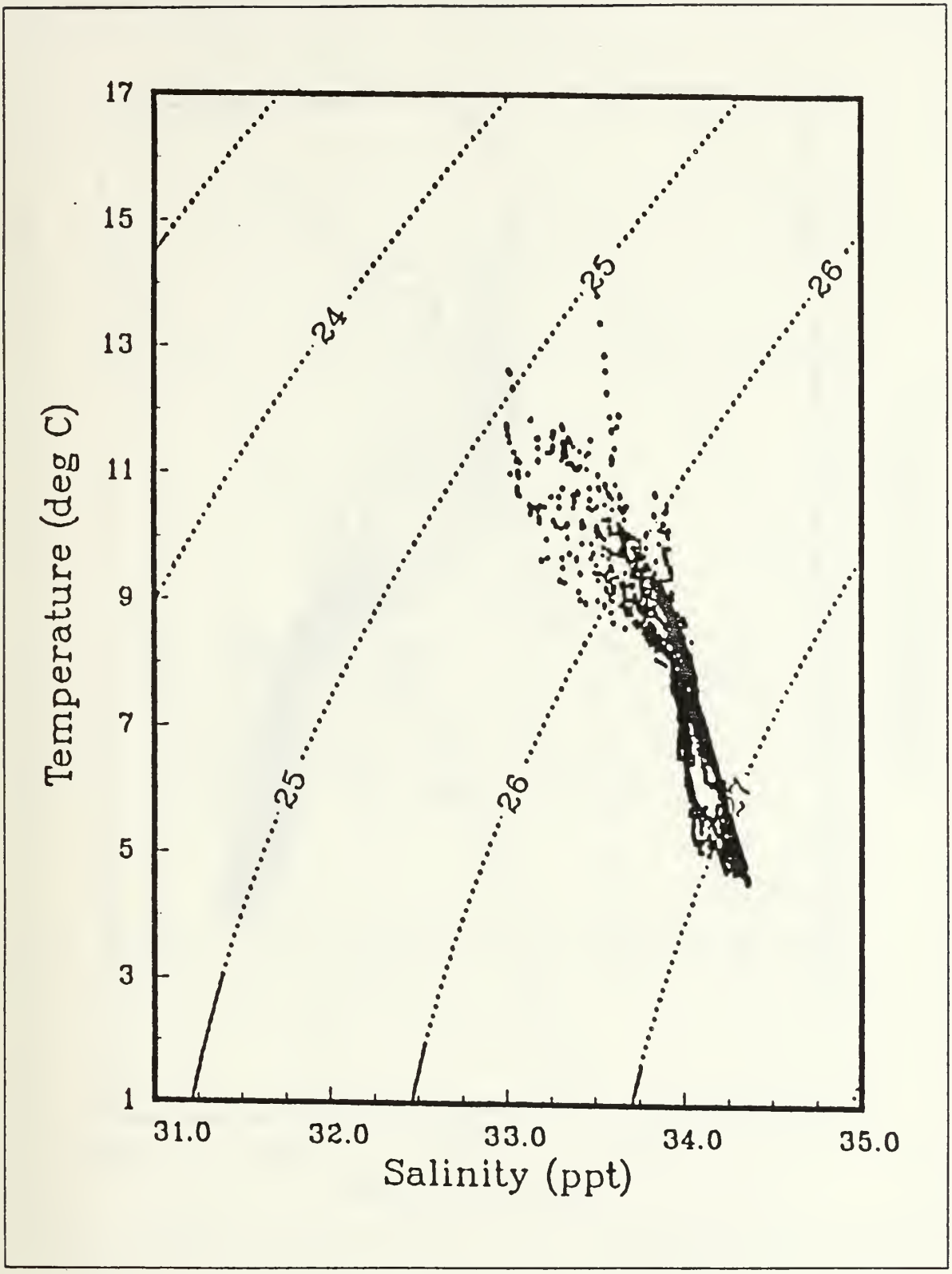

Figure 3.18 OPTOMA 21 nearshore temperature-salinity diagram.

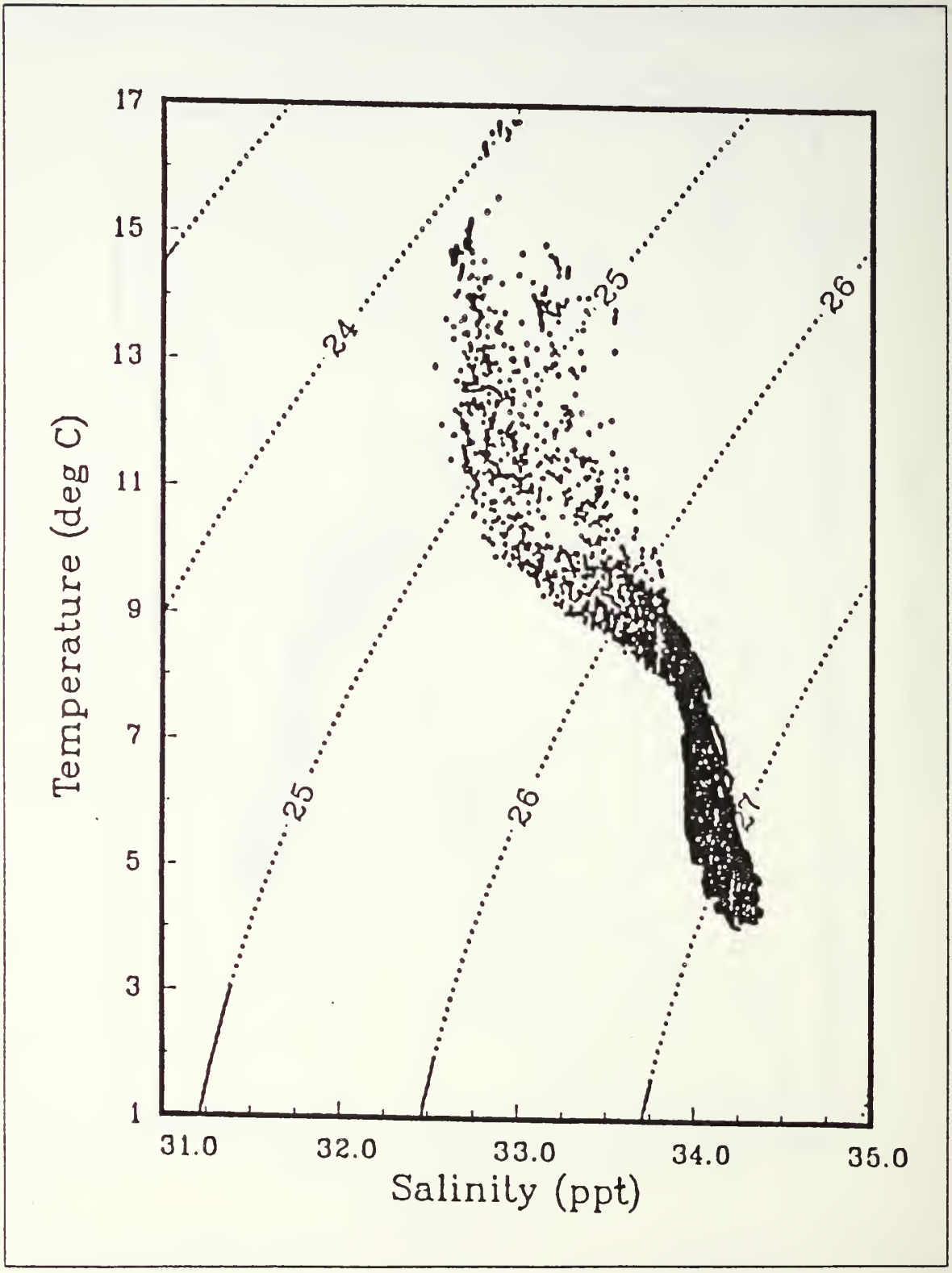

Figure 3.19 OPTOMA 21 offshore temperature-salinity diagram.

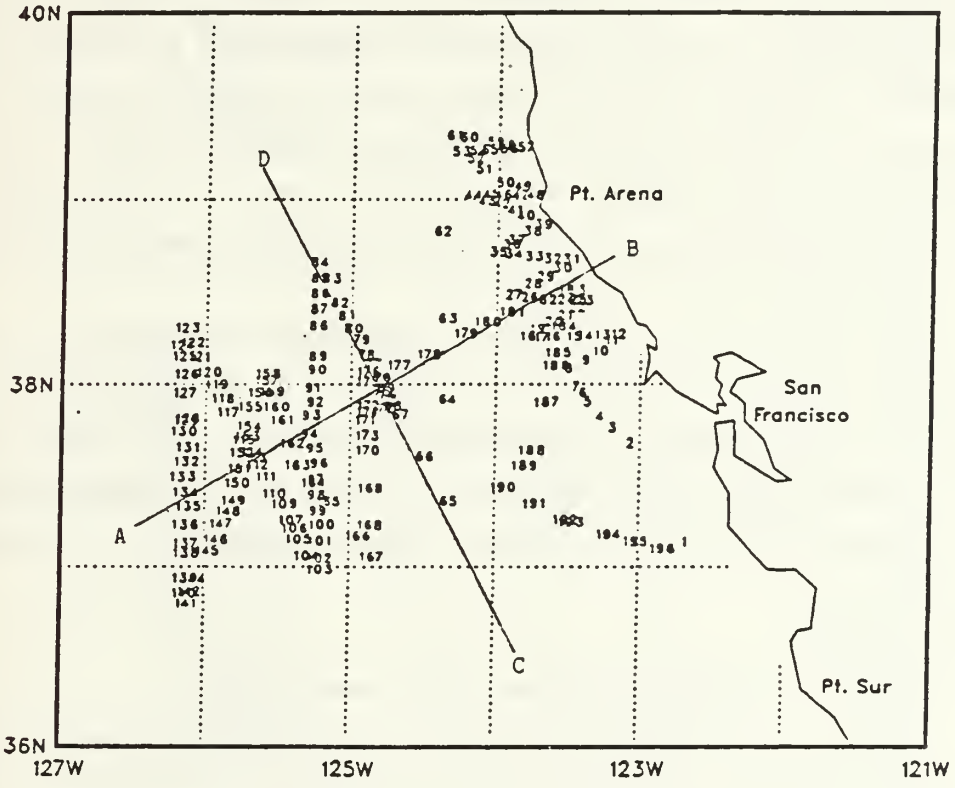

Figure 3.20 Survey stations for OPTOMA 21 (from Wittmann *et al.*, 1987) and the two vertical cross sections.

The salinity cross section (Figure 3.21 b) is consistent with the temperature cross section. Down to ~150 m the isohalines tilt toward the surface indicating upwelling of salty water. Offshore below ~150 m at station 114, the isohalines show a region of 'fresh' water. Along the coast below ~100 m, the isohalines tilt down toward the coast, indicating 'fresh' water. The fresh and warm subsurface coastal waters are likely part of the poleward flowing undercurrent (Chelton, 1984).

The cross jet vertical cross section, C-D, is shown in Figure 3.22. The contour interval for the two cross sections is the same as for the along jet cross sections. The temperature cross section (Figure 3.22 a) indicates generally cool surface and near surface temperatures at stations 65, 66, 67, and 76. Station 76 is in the southwest-oriented jet as seen by the relatively low temperatures at the surface and 50 m. Otherwise, aside from a 'warm' reading at the 50 m depth of station 66, the isotherms down to 150 m show little fluctuation. Below this depth the northern stations (82 and 84) and southern stations (65, 66, and 67) indicate cold water. Stations 76 and 79 reveal warmer water. This infers an anticyclonic flow centered on station 79 below 250 m.

The salinity vertical cross section (Figure 3.22 b) reveals the maximum surface salinity (33.21‰) at station 66. This appears to be the top of a salinity maximum 'dome' that is better seen between 100 m and 500 m. This 'dome' correlates extremely well with the 26 dyn-cm contour on the 250 m dynamic height chart (Figure 3.17 a). A surface salinity minimum (32.61‰) is seen at station 79, on the north side of the upwelled jet.

2. **OPTOMA 22**

a. Dynamic Topography and Geostrophic Current Analysis

Figures 3.23 – 3.28 show the dynamic topography and geostrophic currents of the domain produced by the objective analysis technique for OPTOMA 22 from the XBT soundings. These plots are at the same depth interval and reference level as those for OPTOMA 21. The dynamic topography at the surface (Figure 3.23 a) indicates the flow is along the coast vice perpendicular to the coast as seen in the surface topography from OPTOMA 21. The nearshore topographic field is dominated by two anticyclones, one north of Point Arena and one outside San Francisco Bay. Separating this nearshore field and the offshore field are two weak cyclones, off Point Arena and San Francisco Bay. Offshore ~150 km the contours parallel the coast, building 15 to 20 dyn-cm to a strong high west-southwest of San Francisco Bay and a

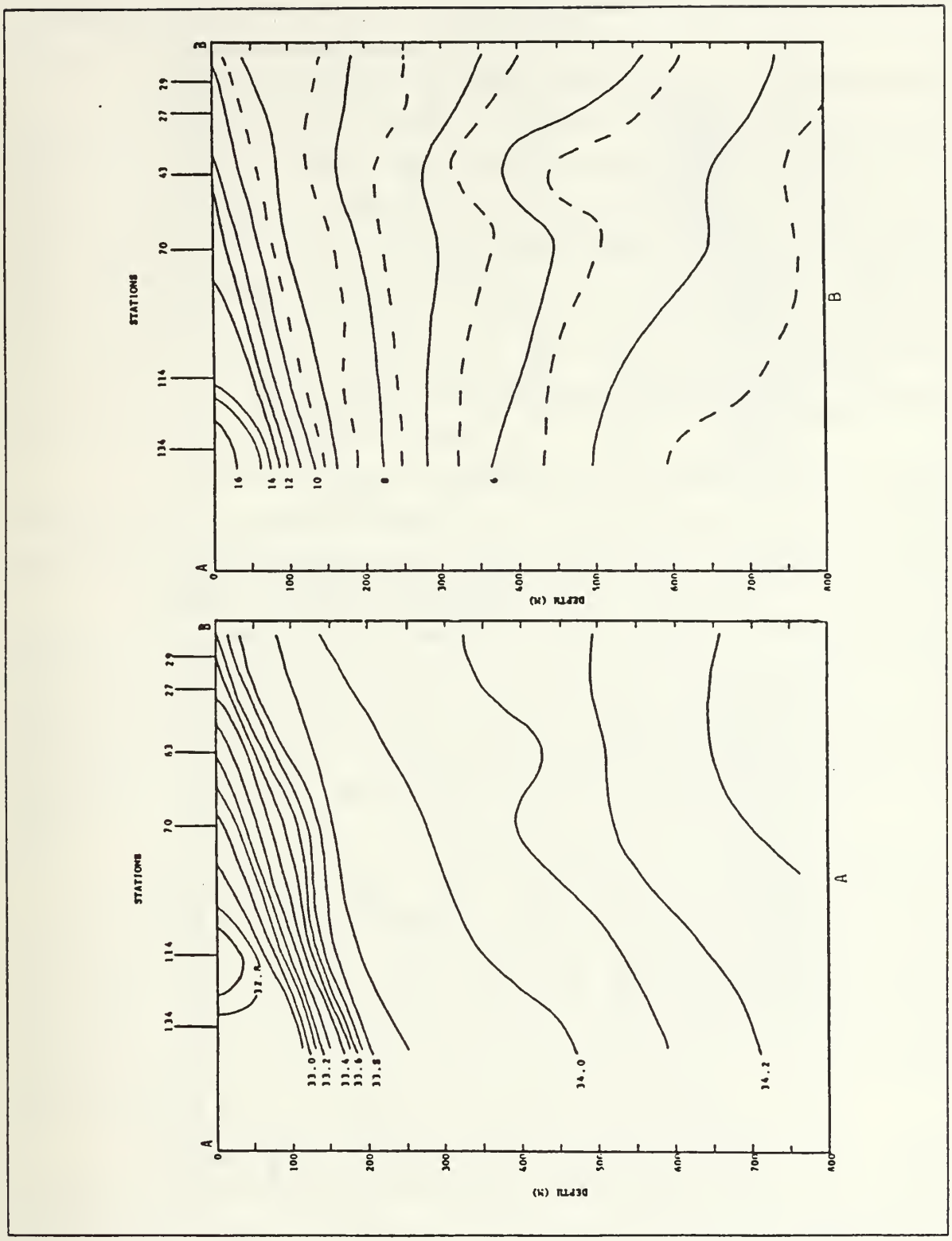

Figure 3.21 OPTOMA 21 vertical cross sections along the jet (A) Temperature and (B) Salinity.

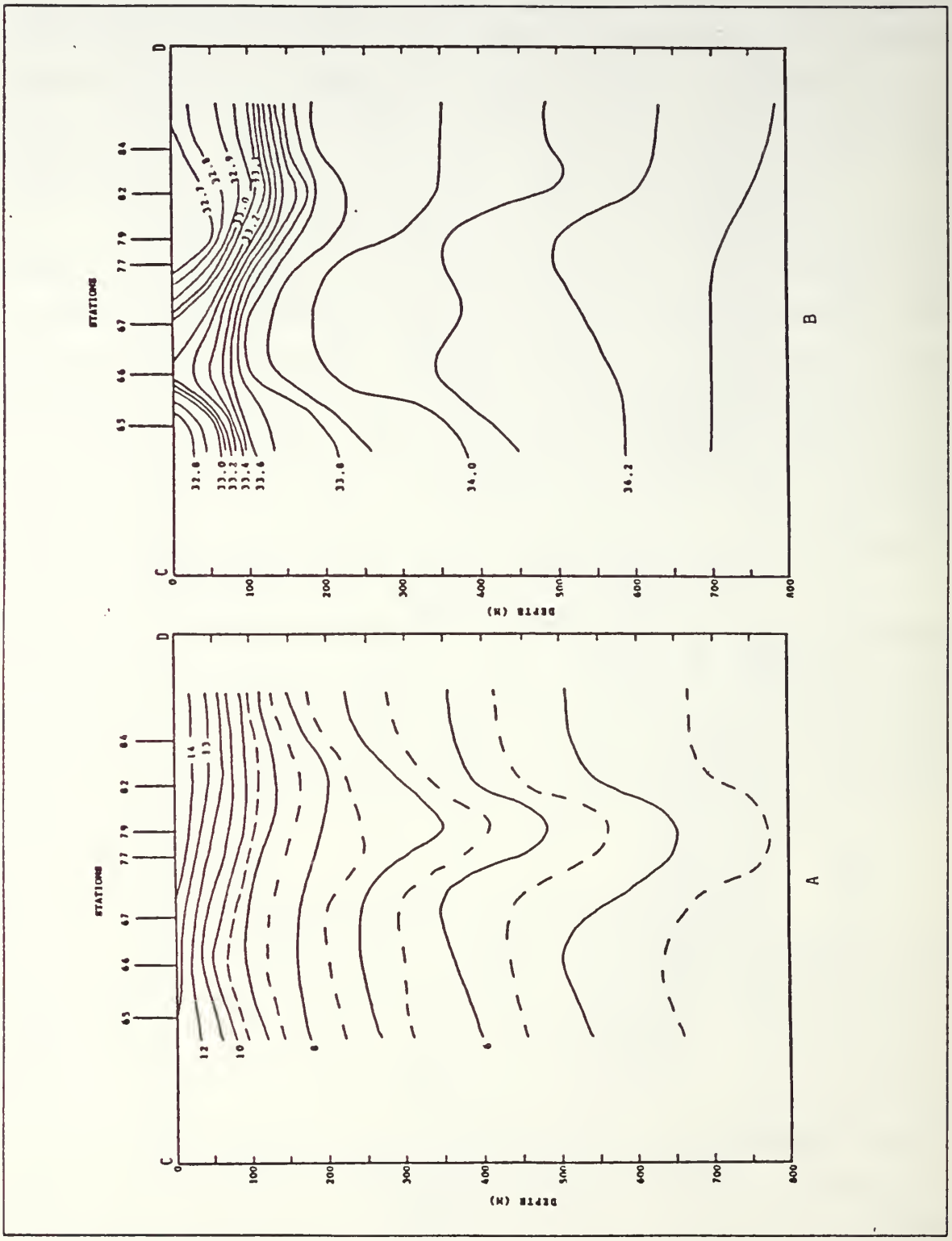

Figure 3.22 OPTOMA 21 vertical cross sections across the jet (A) Temperature and (B) Salinity.

weak high west-southwest of Point Arena. Directly southwest of the latter high is a strong low. Weak lows are also seen in the plot.

The geostrophic current plot (Figure 3.23 b) shows that the general flow is along the coast. The nearshore currents are northward around the two anticyclones at Point Arena and San Francisco Bay. The maximum northward currents off San Francisco Bay are ~25 cm/s, with those off Point Arena reaching a maximum of ~15 cm/s. The obvious feature of the plot is the strong southward flow ~150 km offshore. The southward current maximum varies from ~35 cm/s on the north end of the domain to ~30 cm/s on the south end. Seaward of the southward current is a cyclone to the north and an anticyclone to the south. The cyclonic maximum current velocities are ~30 cm/s at the seaward portion of the flow, with the maximum current velocities for the anticyclonic flow being ~15 cm/s.

In essence, the dynamic topography at 50 m (Figure 3.24 a) is consistent with that seen at the surface in Figure 3.23 a. The relative positions of the highs and lows are the same as the surface with no major deviations in their strengths discernible.

Likewise, the geostrophic currents (Figure 3.24 b) indicate a flow field very similar to the surface flow field. Maximum current velocities for the two highs off Point Arena and San Francisco Bay are ~15 cm/s and ~25 cm/s, respectively. The offshore southward flow maximum at the north end of the domain is ~25 cm/s, and ~20 cm/s at the south end. The cyclonic flow current maximum is ~25 cm/s, and again at the seaward flow. The maximum current for the anticyclonic flow is ~20 cm/s.

Figures 3.25 a – 3.28 a all show the same basic water structure seen above with only minor variations. The noticible difference of the plots with depth is the dynamic low, located southwest of San Francisco Bay, changing from a closed contour low at 100 m to an open contour low at 250 m. The southward offshore flow remains discernible, as does the northward coastal flow. Interestingly, the dynamic height contours indicate a fairly uniform gradient for the 100 and 150 m depths, but at the 200 m and 250 m depths the gradient is strongest in the near coastal field.

The geostrophic currents for 100 to 250 m (Figures 3.25 b – 3.28 b) indicates the northward coastal flow remains strong with depth and dominates the 250 m current field (Figure 3.28 b). Also, the anticyclonic flow west-southwest of San Francisco Bay maintains a strong signature with depth. The maximum northward coastal flow is ~25 cm/s at 100 m, decreasing to ~12 cm/s at 250 m. Maximum speeds for the anticyclonic flow are ~8 cm/s.

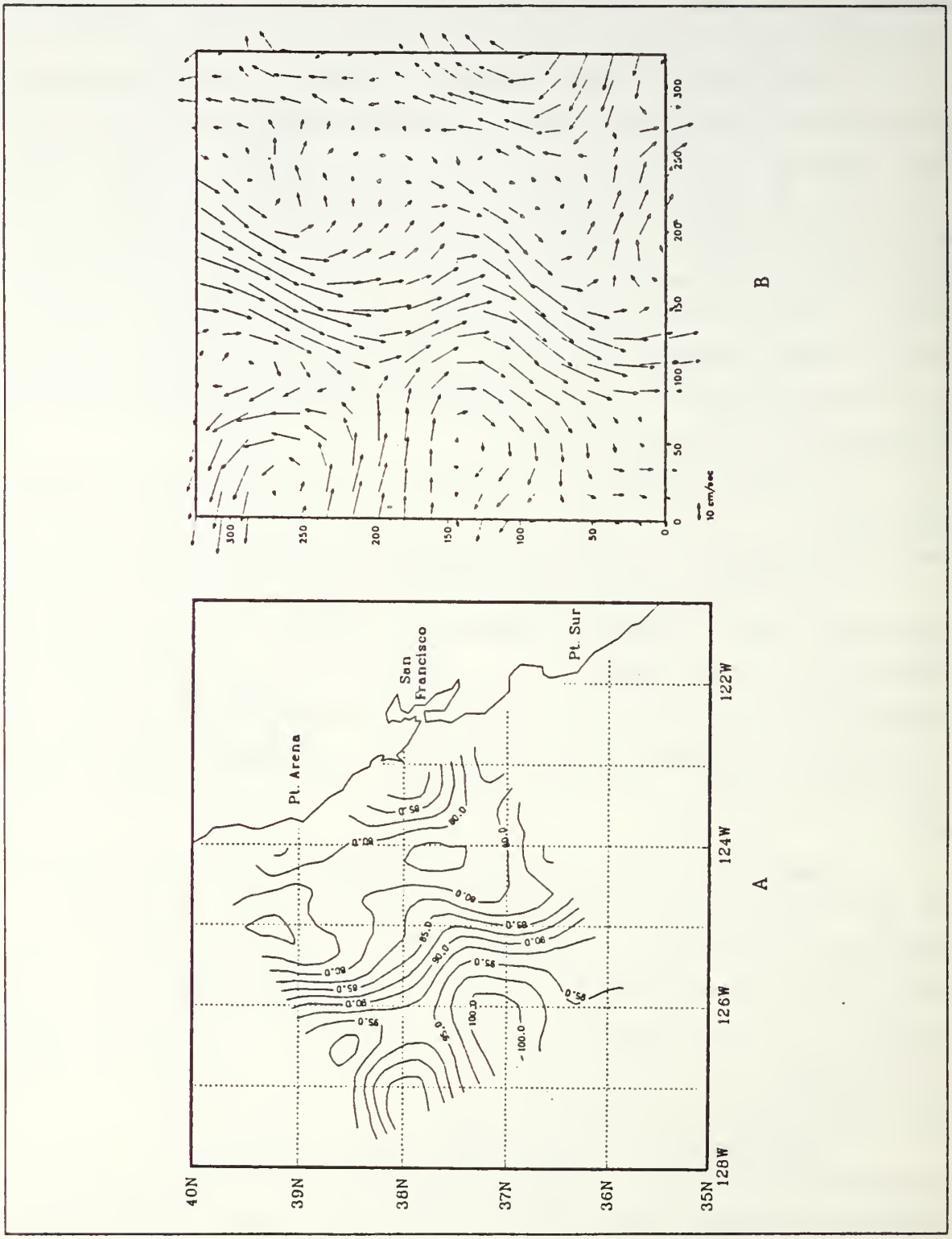

Figure 3.23 OPTOMA 22 (A) Surface dynamic topography and (B) Surface geostrophic currents.

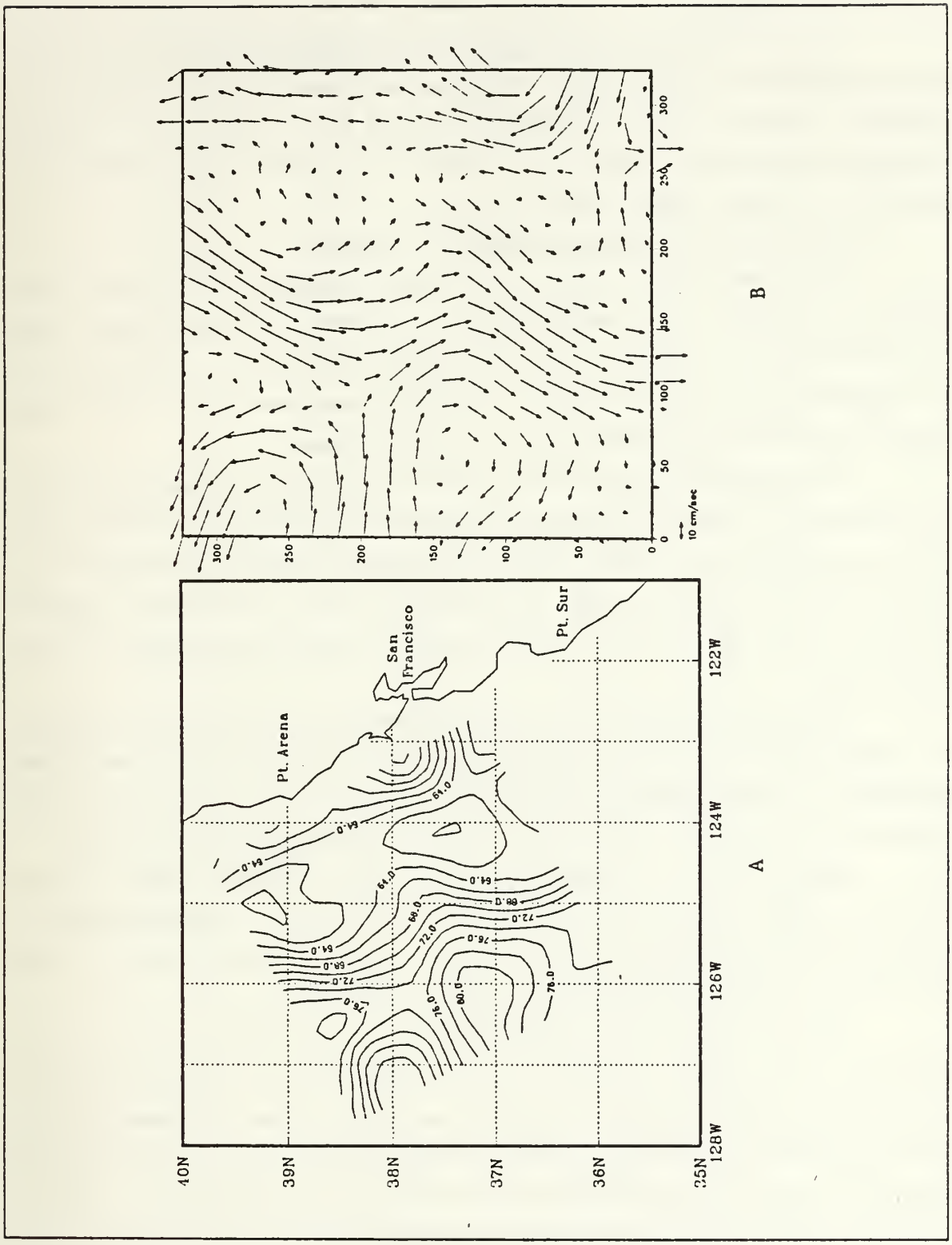

Figure 3.24 OPTOMA 22 (A) 50 m dynamic topography and (B) 50 m geostrophic currents.

b. T-S Diagrams

Figure 3.29 shows the OPTOMA 22 T-S diagram for the offshore CTDs, the only area where CTDs were taken. A comparison of the offshore T-S diagrams for OPTOMA 21 (Figure 3.19) and OPTOMA 22 (Figure 3.29) shows the same range of temperatures and salinities with depth. However, a narrower range of salinites is discernible in the upper layers for OPTOMA 22.

c. Vertical Cross Sections of the OPTOMA 22 Domain

Four vertical cross sections were drawn across the southern half of the OPTOMA 22 domain. Like the OPTOMA 21 cross sections, these are drawn from XBT and CTD data to a depth of 750 m. No salinity cross sections are shown due to the general lack of CTD data (only six CTD casts were made due to heavy seas). Figure 3.30 shows where the sections were taken in the domain.

The temperature vertical cross section taken along the southern boundary of the domain, E-F, is seen in Figure 3.31. The increase in tilt of the isotherms near the surface indicates only a slight increase in upwelling. At 100 m the signature of a dome of cold water becomes evident at stations 176 – 182. This cold water dome is visible down to the 750 m depth. On either side of the cold water are areas of much warmer water.

Section G-H, Figure 3.32, is a cross section taken ~50 km north of section E-F. Figure 3.32 is very similar to section E-F. The obvious feature is the cold water dome below 100 m from station 174 to station 73. At the coast below 100 m the water is again warm. Warm water is seaward of the cold dome, particularly below 300 m.

Along section I-J the tilt of the near surface isotherms indicates broad upwelling at stations 101 and 76 (Figure 3.33). As with the cross sections before, a cold dome is obvious in the diagram but is now centered sharply on station 101. The warm water of a poleward undercurrent is seen below 100 m.

Figure 3.34 shows the vertical cross section of OPTOMA 22, K-L, which corresponds to the along jet cross section of OPTOMA 21, A-B (Figure 3.21). Comparing the two cross sections, two points are obvious. First the general upward tilt of the isotherms toward the coast remains (although not as much so in OPTOMA 22). Also the surface and near surface water in section K-L are dramatically warmer. This difference is primarily at the surface and at 100 m and is 2 to 5 K warmer than section A-B. In section K-L the cold dome does not display the strong signature as in the southern sections, but is still evident below 150 m. Likewise the poleward undercurrent is recognizable below 200 m next to the coast.

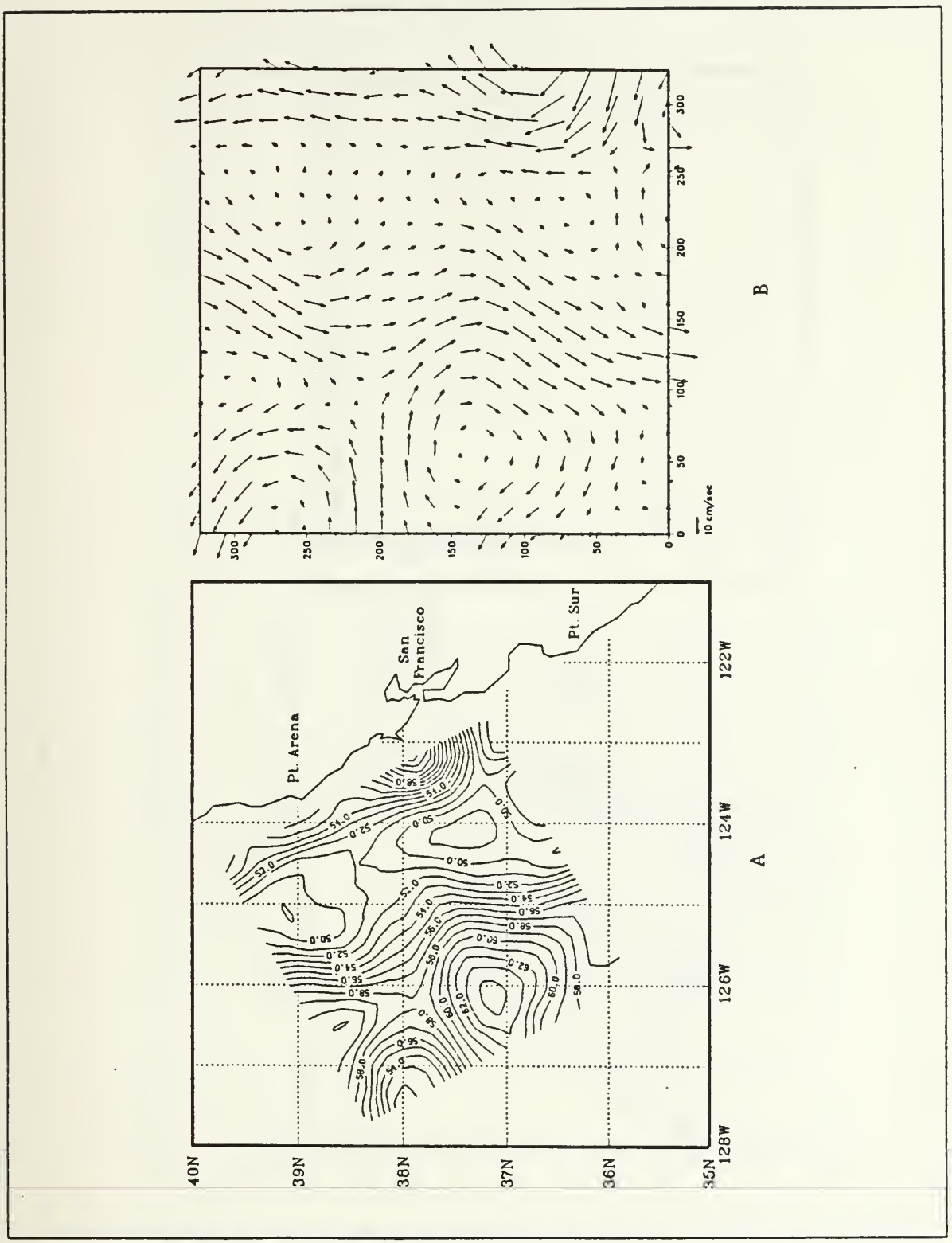

Figure 3.25 OPTOMA 22 (A) 100 m dynamic topography and (B) 100 m geostrophic currents.

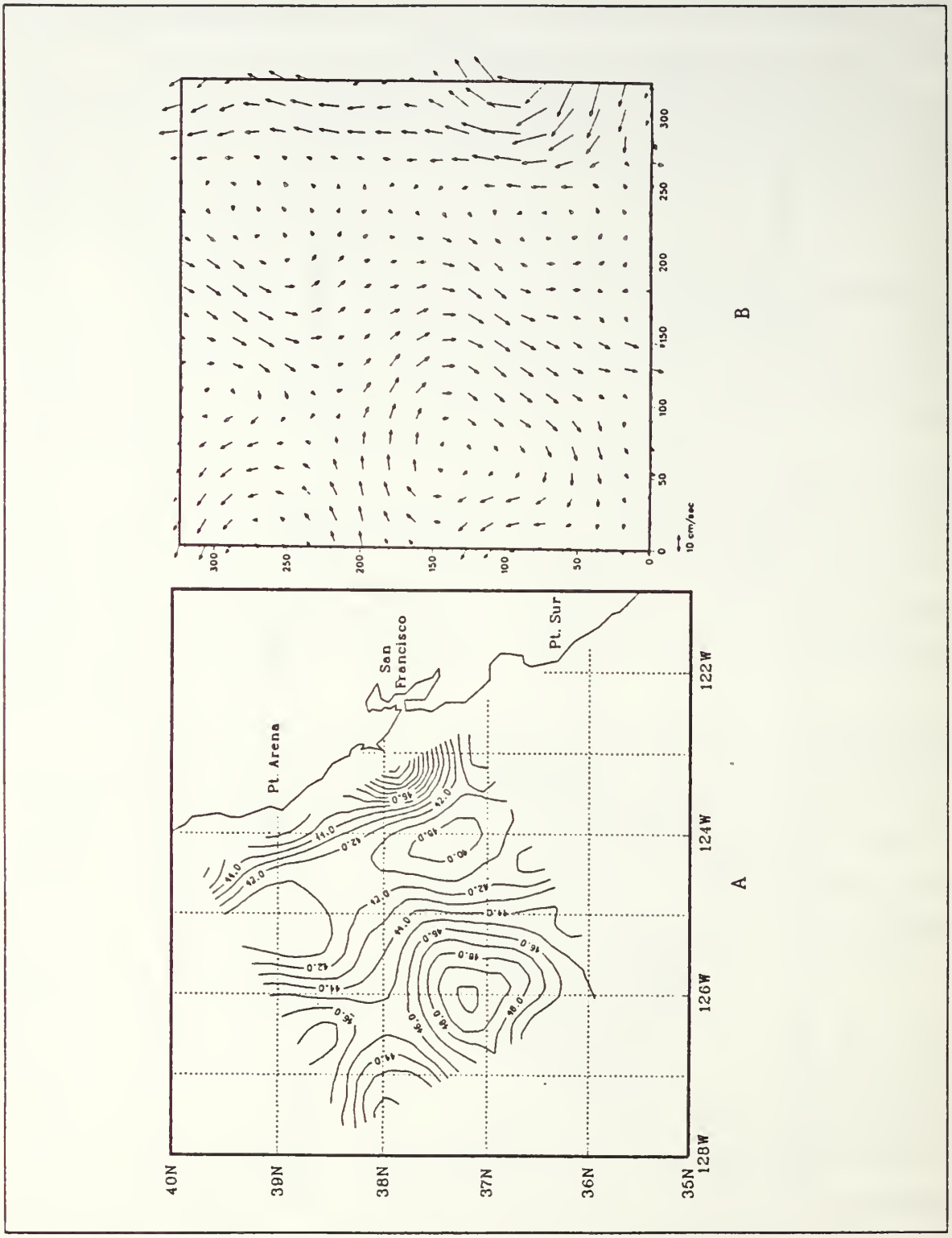

Figure 3.26 OPTOMA 22 (A) 150 m dynamic topography and (B) 150 m geostrophic currents.

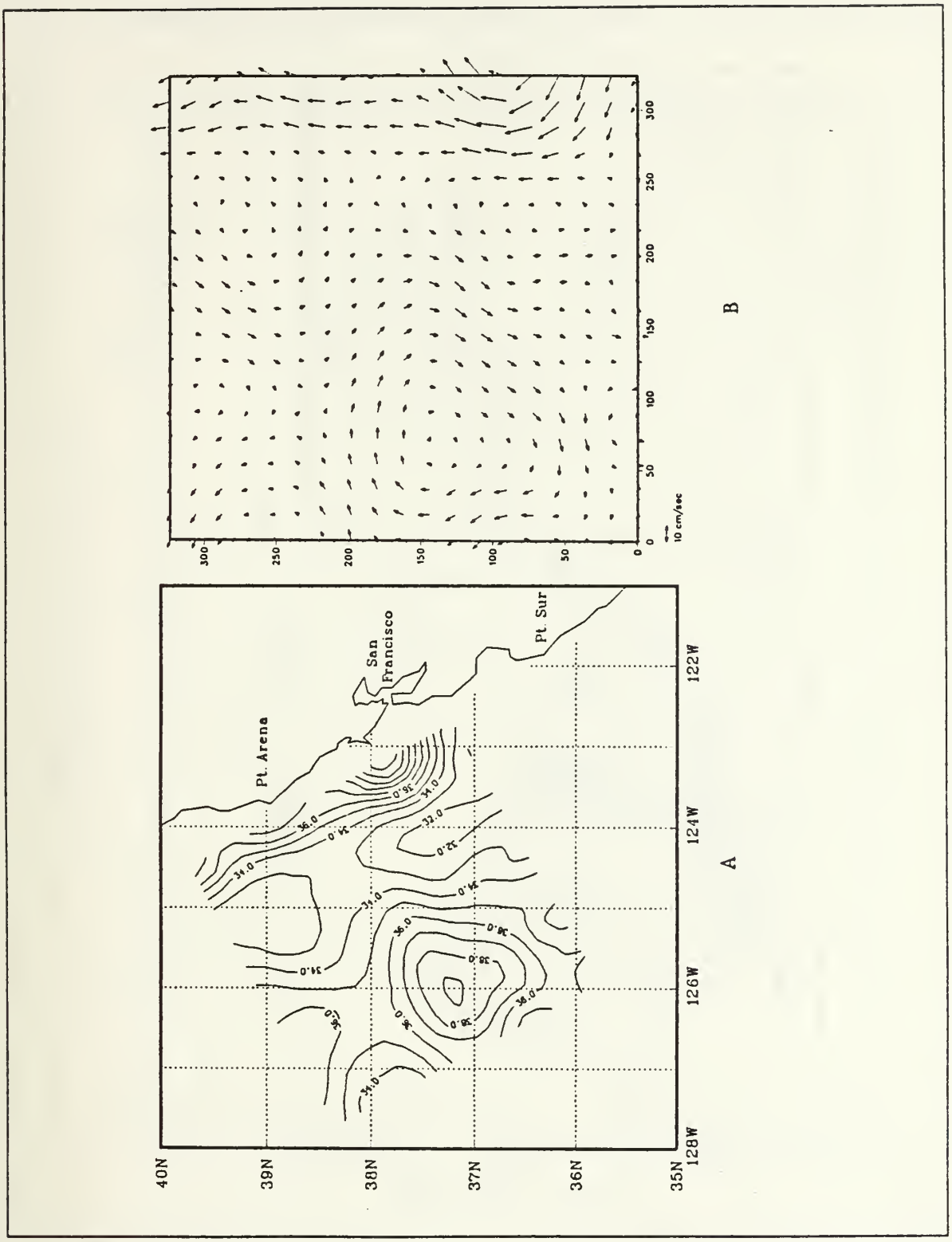

Figure 3.27 OPTOMA 22 (A) 200 m dynamic topography and (B) 200 m geostrophic currents.

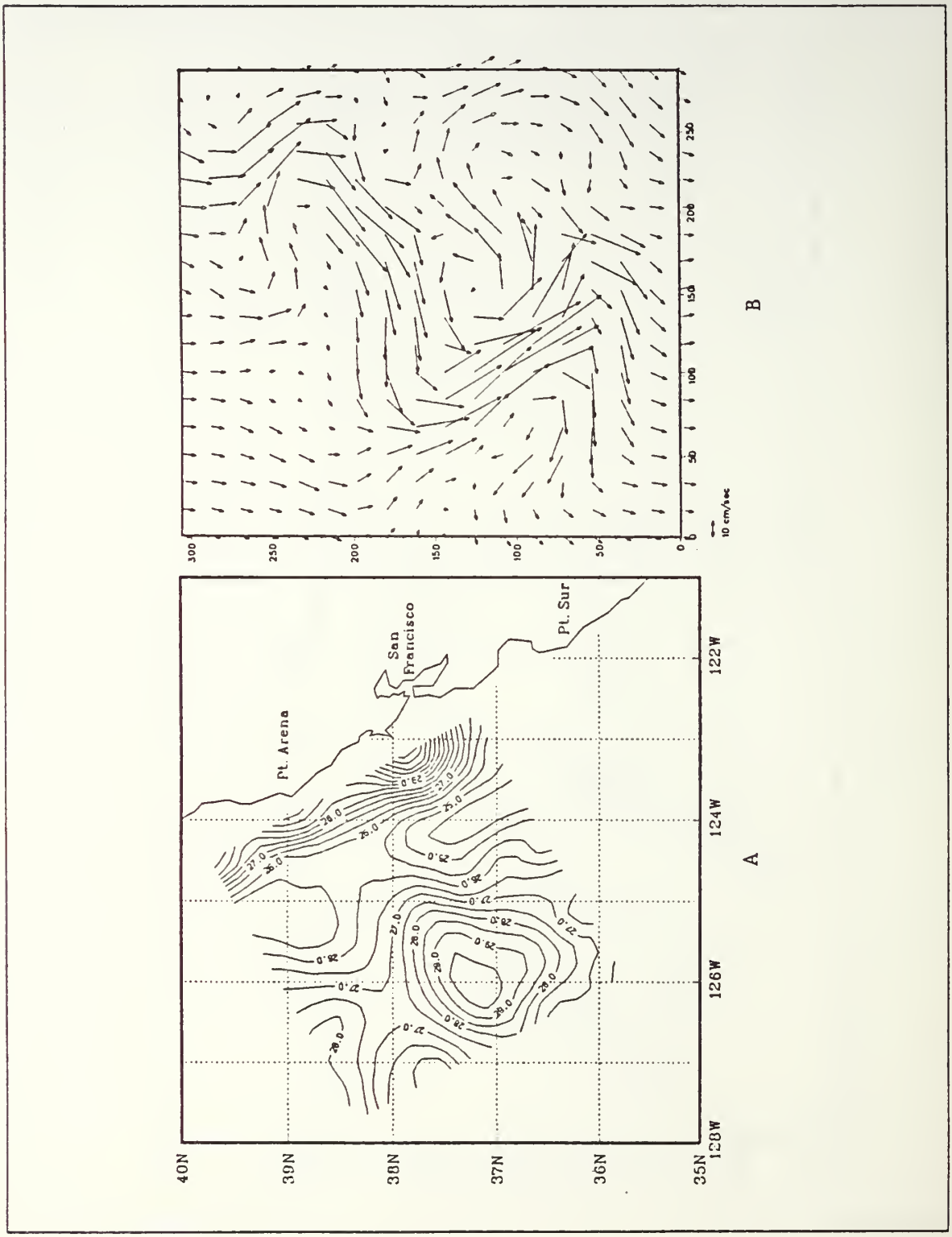

Figure 3.28 OPTOMA 22 (A) 250 m dynamic topography and (B) 250 m geostrophic currents.

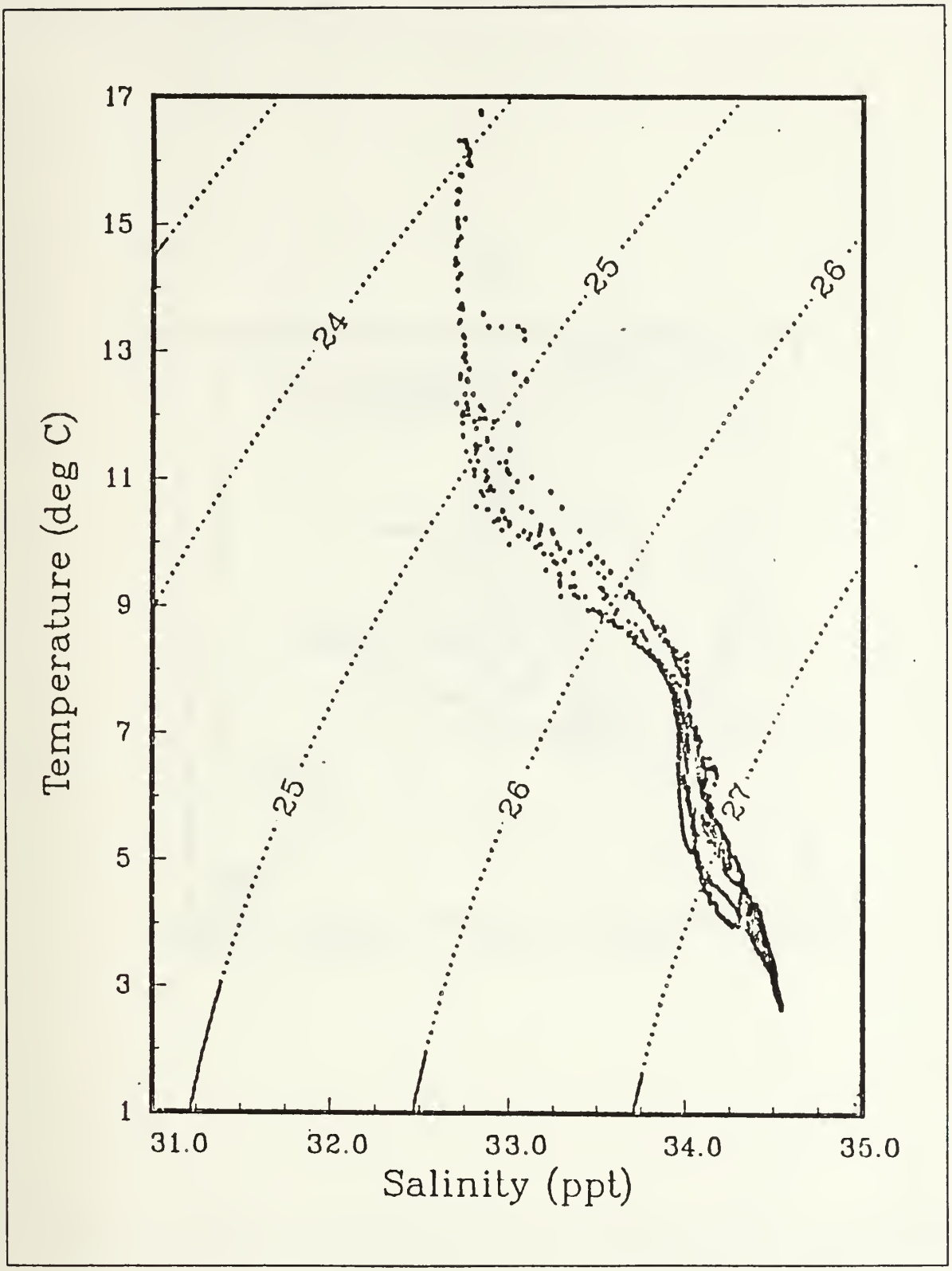

Figure 3.29 OPTOMA 22 offshore temperature-salinity diagram.

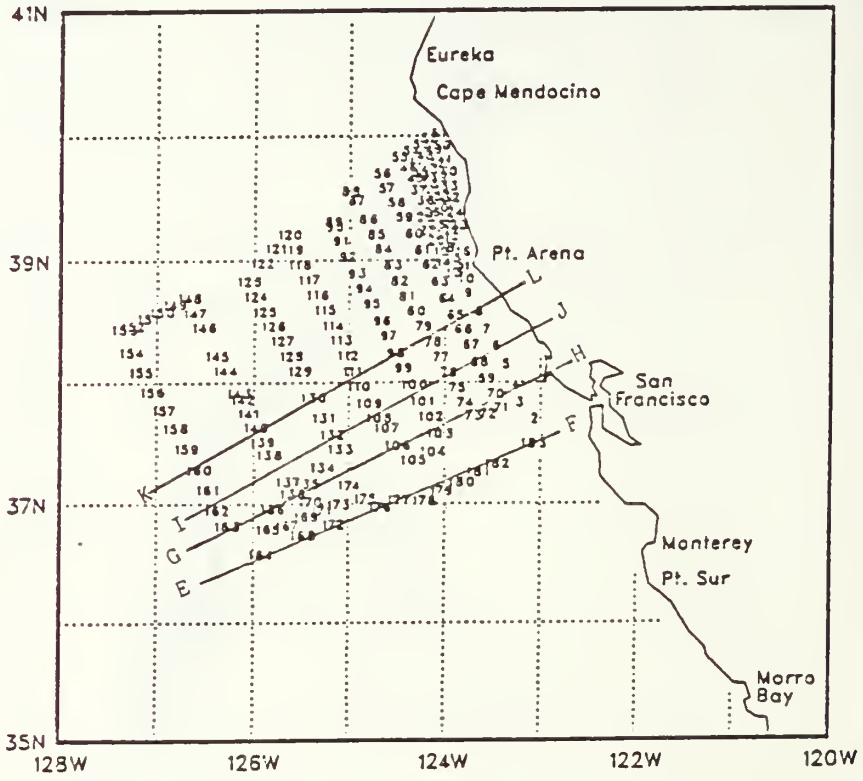

Figure 3.30 OPTOMA 22 stations and the vertical cross sections (from Ciandro *et al.*, 1986).

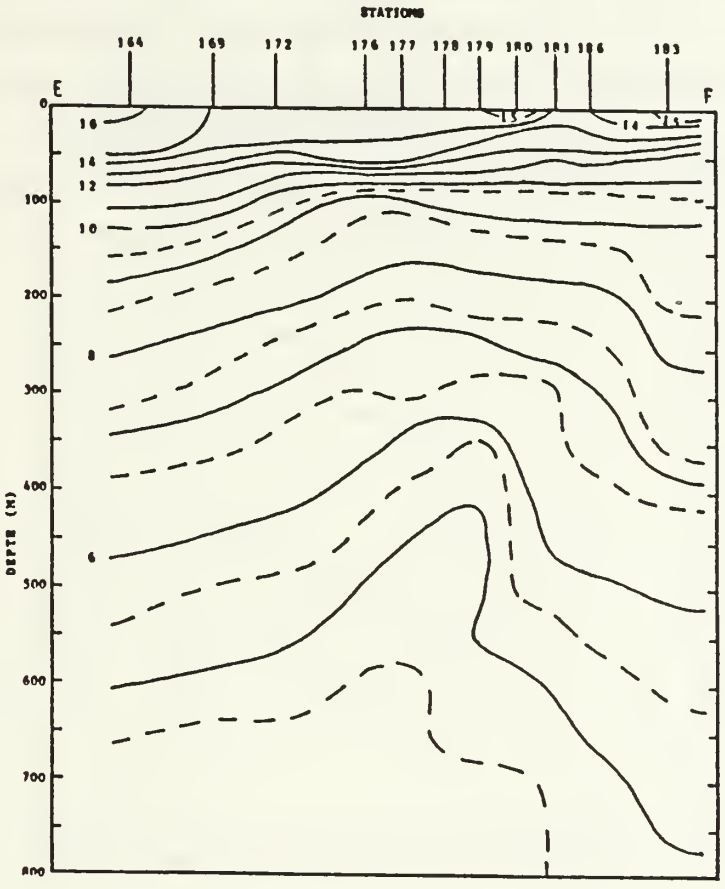

Figure 3.31 OPTOMA 22 temperature vertical cross section at E-F.

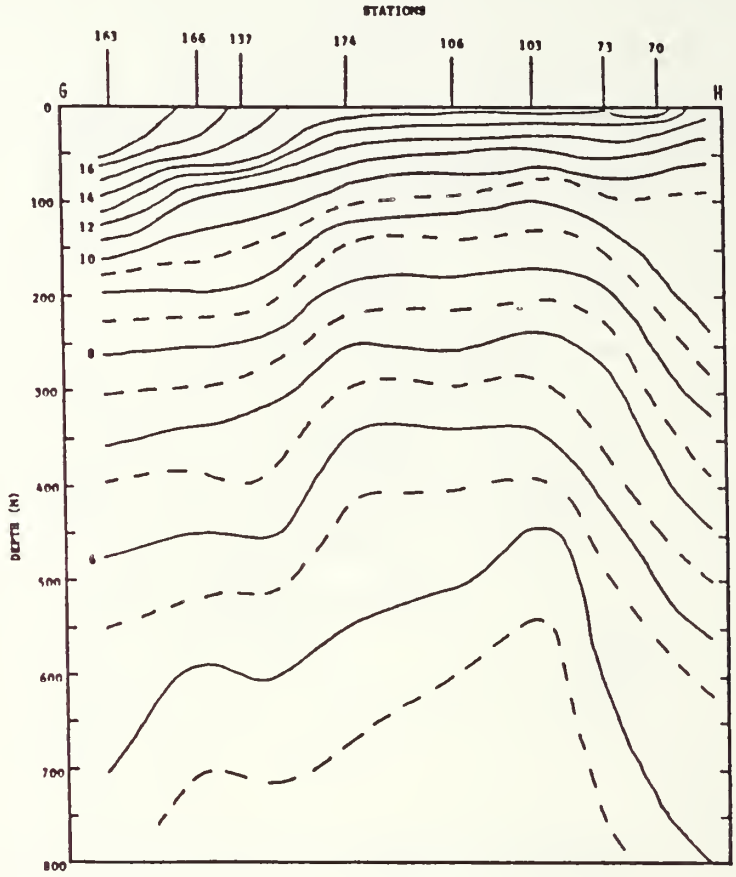

Figure 3.32 OPTOMA 22 temperature vertical cross section at G-H.

3. Coastal Flow

The dynamic topography maps and geostrophic currents of OPTOMA 22 (Figures 3.23 – 3.28) indicate a northward coastal flow. Maps of the coastal SST (Figures 2.2 and 2.4). also indicate substantial increases in the SST fields from OPTOMA 21 to OPTOMA 22

This alongshelf poleward current and warming appears to be associated with the wind reversals noted prior to and during OPTOMA 22 and with solar heating. Send *et al.*, (1987) concluded that wind relaxations have a tendency to cause the inner shelf currents to flow poleward, vice the dominant southward coastal flow seen during equatorward winds. They further state that surface heating is a result of solar heating and alongshore advection. Normally the surface heating would not be noticed since it would be balanced by the upwelling of cold water.

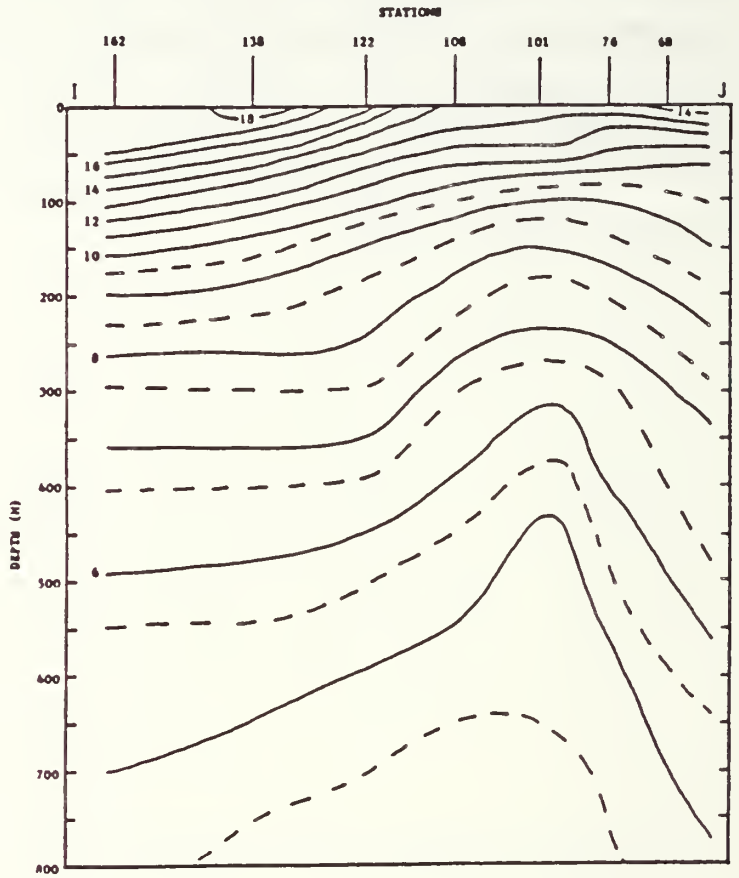

Figure 3.33 OPTOMA 22 temperature vertical cross section at I-J.

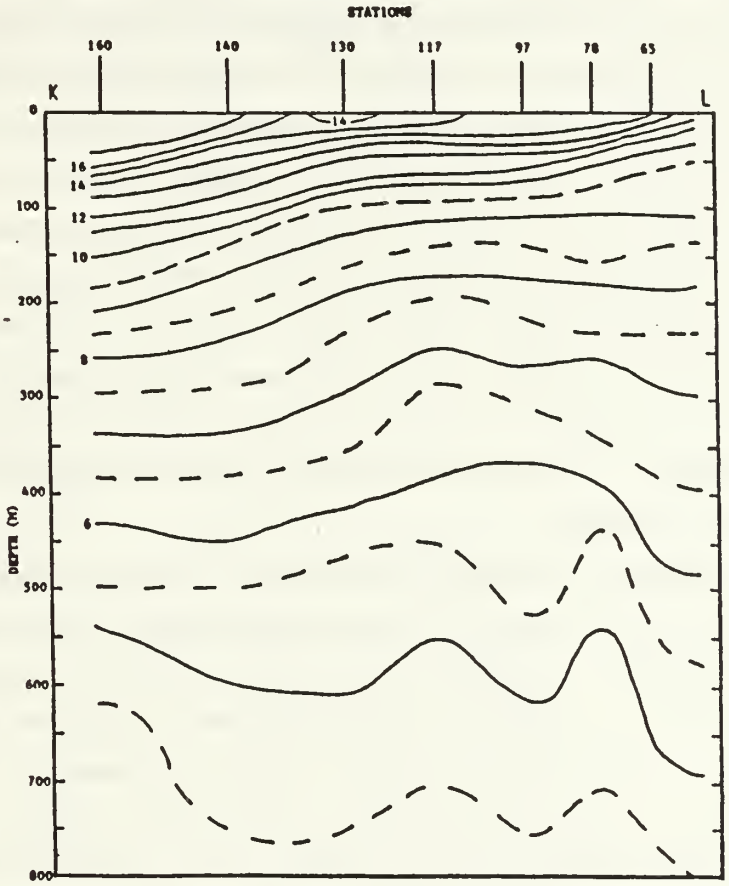

Figure 3.34 OPTOMA 22 temperature vertical cross section at K-L.

IV. CONCLUSIONS AND RECOMMENDATIONS

A. CONCLUSIONS

This study has examined changes in the CCS south of Point Arena, California. During the time frame 7 July – 5 August 1986, the winds changed from a dominant equatorward regime to one of both poleward and equatorward fluctuations.

The winds were favorable for upwelling for the time frame through, and just beyond, the OPTOMA 21 cruise. However, following the OPTOMA 21 cruise, the winds changed dramatically in speed, direction, or both. The winds became either weakly favorable or not at all favorable for upwelling. This had a pronounced impact on the nearshore flow, resulting in a northward flow pattern very similar to that seen during the CODE project during 1982. Winant (1987) and Kosro (1987) both concluded that, in the absence of an wind forcing, a northward coastal flow would be seen between Point Reyes and Point Arena. Associated with this northward coastal flow is coastal warming, which is a result of solar heating of the inner shelf waters and subsequent northward advection.

The offshore flow field is more perplexing though. The only reliable wind data is from buoy NDBC 14 which is relatively nearshore (see Figure 2.5). A drastic change did take place in the offshore flow field, a change that turned the 'perpendicular to the coast' flow to a 'parallel to the coast' flow. The mechanics of what caused this change are not well known. Although it is possible that the surfacing of the poleward undercurrent could be the cause, since Figure 3.23 indicates surface poleward flow, analysis of cross-sections of the poleward undercurrent (e.g., Figure 3.31) indicate that it remained subsurface throughout the cruises. It is possible that the northward winds (i.e. wind reversals) observed from NDBC 14 prior to and during OPTOMA 22 could be associated with the changes seen in the flow patterns of the CCS.

B. RECOMMENDATIONS

This paper, as well as the CODE papers, described the change of the current structure (upwelling versus non-upwelling events) during a variety of wind conditions. Both also studied the effects of a changing wind field on the coastal waters. However, all of this was done as a consequence of analysis after the fact. By this I mean research was not done specifically with a wind reversal or wind relaxation event in

mind. These events were found after reviewing the data available. Therefore, a study should be initiated to research the closeknit relationship between winds parallelling the coast and coastal upwelling or water column mixing. This should be conducted in a geographical area known for its strong alongshore wind stress and the associated upwelling and should be able to account for the offshore water structure changes. One strong candidate for this domain would be in and around the OPTOMA NOCAL and CODE domains because upwelled jets appear "to be geographically 'anchored' to capes or points in regions of strong coastal winds" (Brink and Hartwig, 1985).

One method, which is likely to be expensive, would be to set out an x-shaped pattern of current meter moorings oriented parallel/perpendicular to the coast. Preferably, ten moorings spaced less than 20 km apart would be placed in a line parallel to the coast approximately 120 km offshore. Ten moorings would then be placed in a line perpendicular to the coast centered on the above line. The moored buoys would have current meters at equal (say 25 m) intervals from the surface to the main thermocline. Ideally meteorological buoys (collecting wind direction and speed data) would be positioned in the middle of the pattern and at each end of the array. This pattern should ideally be "centered on the historical" (Brink and Hartwig, 1985) upwelling filament off Point Arena. The current meter network would be in place and acquiring data during the upwelling season. If there is no regional scale phenomenon present (Halliwell and Allen, 1987), this would allow data acquisition during times of upwelling and would truly document a fall transition when winds favorable for upwelling reverse. This would ideally allow the best temporal scale for observations.

Another recommendation would be to use aircraft utilizing air-dropped XBT's (AXBT's). These flights could be spaced at two-day intervals to preserve temporal continuity. Again, these would be carried out during a wind reversal in order to obtain the necessary oceanographic data. The wind data could be obtained from NDBC 14, the meteorological buoy located off Point Arena.

If aircraft support is not available, underway surveys with a Doppler Acoustic Log (DAL) profiling the subsurface currents could be conducted. Due to planning, cost and lead time restraints, the surveying should be conducted throughout the upwelling season until a wind reversal and the subsequent water structure change was recorded. For this planning phase, historical reports should be examined for indications of wind reversals since they tend to occur with little notice and last for periods of hours to one or two days (Dorman, 1987). Since the reversals are usually

linked to anomolous atmospheric conditions for the time of year (i.e., troughs or lows moving through the area), a constant vigil on the weather for the domain may be required. This information could easily be sent to a ship to ensure the ship is ready for a change in weather condition. The cruises would be long, possibly a month at a time to permit continuity, and would be conducted from ~March through September, the upwelling 'season'. If this is not possible, surveys could be made with shorter time intervals (i.e., days) separating them.

Of course, it is assumed that satellite support would be used on these moored current meter/flight/cruise data studies. Even though the area around Point Arena is plagued with low clouds during the upwelling season, satellite support, when available, would provide an important source of oceanographic data.

LIST OF REFERENCES

Bakun, A., 1973: Coastal upwelling indices, west coast of North America, 1946-1971. *S.S. Dept. Commer., NNOAA Tech. Rep. NMFS SSRF-671*, 103pp.

Bakun, A., 1975: Daily and weekly upwelling indices, West Coast of North America, 1967-1973. *U.S. Dept. Commer., NNOA Tech. Rep. NMFS SSRF-693*, 114pp.

Bakun, A., 1986: Upwelling index update, U.S. West Coast, 33°N- 48°N Latitude. *U.S. Dept. Commer., NNOA-TM-NMFC-67*, 81pp.

Beardsley, R.C. and S.J. Lentz, 1987: The Coastal Ocean Dynamics Experiment Collections: An Introduction. *J. Geophys. Res.*, **92**, 1455-1463.

Bernstein, R.L., L.C. Breaker and R. Whritner, 1977: California Current eddy formation: Ship, air, and satellite results. *Science*, **195**, 353-359.

Bretherton, F.P., R.E. Davis and C.B. Fandry, 1976: A technique for objective analysis and design of oceanographic experiments applied to MODE-73. *Deep-Sea Res.*, **3**, 559-582.

Brink, K.H. and E.O. Hartwig, 1985: *Coastal Transition Zone Workshop Report*, Office of Naval Research, 67pp.

Bucklin, A., 1986: Allozymes as indicators of biological/physical interactions (OPTOMA 21). *Trans. Am. Geophys. Union*, **67**, 1048.

Carter, E.F. and A.R. Robinson, 1981: Time series of synoptic maps of the western North Atlantic; A space-time objective analysis of POLYMODE XBT's. *Reports in Meteorology and Oceanography*, Number 15, Division of Applied Sciences, Harvard Univer., 14pp.

Chelton, D.B. 1984: Seasonal variablity of alongshore geostrophic velocity off central California. *J. Geophys. Res.*, **89**, 3473-3486.

Ciandro, M.L., P.A. Wittmann, A.A. Bird and C.N.K. Mooers, 1986: Hydrographic Data from the OPTOMA program; OPTOMA 22. *NPS Technical Report, NPS-68-86-012*, Naval Postgraduate School, Monterey, California, 41 pp.

Dorman, C.E., 1985: Hydraulic Control of the Northern California Marine Layer (abstract), *Eos Trans*, AGU, **66**, 914.

Dorman, C.E., 1987: Possible Role of Gravity Currents in Northern California's Coastal Summer Wind Reversals. *J. Geophys. Res.*, **92**, 1497-1506.

Flegal, A.R., 1986: OPTOMA 21: Lead Isotope Systematics of an Oceanic Jet. *Trans. Am. Geophys. Union*, **67**, 1048.

Gandin, L.S., 1965: Objective Analysis of Meteorological Fields, Israel Program for Scientific Translations, Jerusalem, 242pp.

Halliwell, G.R., Jr., and J.S. Allen, 1987: The Large-Scale Coastal Wind Field Along the West Coast of North America. *J. Geophys. Res.*, **92**, 1861-1884.

Hickey.B.M., 1979: The California Current System: hypothesis and facts. *Prog. in Oceanogr.*, **8**, 191-279.

Huyer, A., 1983: Coastal upwelling in the California Current System. *Prog. in Oceanogr.*, **12**, 259-284.

Huyer, A. and P.M. Kosro, 1987: Mesoscale Surveys Over the Shelf and Slope in the Upwelling Region Near Point Arena, California. *J. Geophys. Res.*, **92**, 1655-1681.

Jones, B.H., T. Stanton and C.N.K. Mooers, 1986: Biological and Chemical Variability Associated with a Cool Filament off Northern California (OPTOMA-21). *Trans. Am. Geophys. Union*, **67**, 1048.

Kosro, P. M., 1987: Structure of the Coastal Current Field off Northern California During the Coastal Ocean Dynamics Experiment. *J. Geophys. Res.*, **92**, 1637-1654.

Mooers, C.N.K. and M.M. Rienecker, 1987: The structure and evolution of a cool filament /offshore system off Pt. Arena in July 1986. IUGG/ UGGI XIX General Assembly, Vancouver, Canada, 9-22 August.

Mooers, C.N.K., M.M. Rienecker and A.A. Bird, 1986: Overview of OPTOMA 21 (7 to 20 July 1986). *Trans. Am. Geophys. Union*, **67**, 1048.

Mooers, C.N.K., and A.R. Robinson, 1984: Turbulent jets and eddies in the California Current and inferred cross-shore transports, *Science*, **223**, 51-53.

Nelson, C.S., 1977: Wind stress and wind stress curl over the California Current. *NOAA Tech. Tep. NMFS SSRF-714*, U.S. Dep. Commer., 87pp.

Reid, J.B., G.I. Roden and J.G. Wyllie, 1958: Studies of the California Current System. *California Cooperative Oceanic Fisheries Investigations*, Progress Report, 1 July 1956 - 1 January 1958, 28-56.

Rienecker, M.M., C.N.K. Mooers, D.E. Hagan and A.R. Robinson, 1985: A cool anomaly off Northern California: An investigation using IR imagery and in situ data. *J. Geophys. Res.*, **90**, 4807-4818.

Rienecker, M.M., C.N.K. Mooers and A.R. Robinson, 1987: Dynamical interpolation and forecast of the evolution of mesoscale features off Northern California. *J. Phus. Oceanogr.*, **17**, 1189-1213.

Send, U., R.C. Beardsley and C.D. Winant, 1987: Relaxation from Upwelling in the Coastal Ocean Dynamics Experiment. *J. Geophys. Res.*, **92**, 1683-1698.

Stanton, T. and L. Washburn, 1986: Velocity Shear and Thermohaline Structure through an Upwelling Filament. *Trans. Am. Geophys. Union*, **67**, 1048.

Washburn, L. and T. Stanton, 1986: Finestructure and mixing activity through an upwelling filament. *Trans. Am. Geophys. Union*, **67**, 1048.

Winant, C.D., R.C. Beardsley, and R.E. Davis, 1987: Moored Wind, Temperature, and Current Observations Made During Coastal Ocean Dynamics Experiments 1 and 2 Over the Northern California Continental Shelf and Upper Slope. *J. Geophys. Res.*, **92**, 1569-1604.

Wittmann, P.A., M.L. Ciandro, A.A. Bird and C.N.K. Mooers, 1987: Hydrographic Data from the OPTOMA program; OPTOMA 21. *NPS Technical Report, NPS-68-001*, Naval Postgraduate School, Monterey, California, 58 pp.

Zemba, J., and C.A. Friehe, 1987: The Marine Atmospheric Boundary Layer Jet in the Coastal Ocean Dynamics Experiment. *J. Geophys. Res.*, **92**, 1489-1496.

INITIAL DISTRIBUTION LIST

		No. Copies
1.	Defense Technical Information Center Cameron Station Alexandria, VA 22304-6145	2
2.	Library, Code 0142 Naval Postgraduate School Monterey, CA 93943-5002	2
3.	Chairman (Code 68Co) Department of Oceanography Naval Postgraduate School Monterey, CA 93943	1
4.	Chairman (Code 63Rd) Department of Meteorology Naval Postgraduate School Monterey, CA 93943	1
5.	Dr. M.L. Batteen (Code 68Bv) Department of Oceanography Naval Postgraduate School Monterey, CA 93943	2
6.	Dr. C.N.K. Mooers, Director Institute for Naval Oceanography Room 322, Bldg. 1100 NSTL, MS 39529	1
7.	Lt Michael E. Beasley 1416 Beech St. Decatur, Al 35601	2
8.	Melissa Ciandro Scripps Institution of Oceanography Scripps Satellite Oceanography Facility Code A-014 La Jolla, CA 92093	1
9.	Dr. Burton H. Jones Allan Hancock Foundation University of Southern California Los Angeles, CA 90089	1

10.	Timothy P. Stanton Department of Oceanography Naval Postgraduate School Monterey, CA 93943	1
11.	Dr. Libe Washburn Ocean Physics Group Center for Earth Sciences University of Southern California Los Angeles, CA 90089	1
12.	Dr. Michele Rienecker Institute for Naval Oceanography Room 322, Bldg. 1100 NSTL, MS 39529	1
13.	Director, Naval Oceanography Division Naval Observatory 34th and Massachusetts Avenue NW Washington, DC 20390	1
14.	Commander Naval Oceanography Command NSTL Station Bay St. Louis, MS 39522	1
15.	Commanding Officer Naval Oceanographic Office NSTL Station Bay St. Louis, MS 39522	1
16.	Commanding Officer Fleet Numerical Oceanography Center Monterey, CA 93943	1
17.	Commanding Officer Naval Ocean Research and Development Activity NSTL Station Bay St. Louis, MS 39522	1
18.	Commanding Officer Naval Environmental Prediction Research Facility Monterey, CA 93943	1
19.	Chairman, Oceanography Department U.S. Naval Academy Annapolis, MD 21402	1
20.	Naval Ocean Research and Development Activity 800 N. Quincy Street Arlington, VA 22217	1

21.	Office of Naval Research (Code 420) 800 N. Quincy Street Arlington, VA 22217	1
22.	Scientific Liason Office Office of Naval Research Scripps Institution of Oceanography La Jolla, CA 92037	1
23.	Commander Oceanographic Systems Pacific Box 1390 Pearl Harbor, HI 96860	1
24.	Commanding Officer Naval Eastern Oceanography Center Naval Air Station Norfolk, VA 23511	1
25.	Commanding Officer Naval Western Oceanography Center Box 113 Pearl Harbor, HI 96860	1
26.	Commanding Officer Naval Oceanography Command Center, Rota Box 31 FPO San Francisco, CA 09540	1
27.	Commanding Officer Naval Oceanography Command Center, Guam Box 12 FPO San Francisco, CA 96630	1
28.	Director of Research Administration Code 012 Naval Postgraduate School Monterey, CA 93943	1

Thesis
B3145
c.1

Beasley
Changes in the California Current System observed off northern California during July-August 1986.

AMERICAN BINDERY
TOPEKA KANSAS

thesB3145
Changes in the California Current System
3 2768 000 78059 7
DUDLEY KNOX LIBRARY